Journal of Sedimentary Research

Journal of Sedimentary Research, 2006, v. 76, 557–574
Research Article
DOI: 10.2110/jsr.2006.046

PROVENANCE AND TECTONIC SETTING OF CLASTIC DEPOSITS IN THE DEVONIAN XICHENG BASIN, QINLING OROGEN, CENTRAL CHINA

ZHEN YAN,[1] ZONGQI WANG,[2] TAO WANG,[2] QUANREN YAN,[2] WENJIAO XIAO,[1] AND JILIANG LI[1]
[1]*State Key Laboratory of Lithospheric Evolution, Institute of Geology and Geophysics, Chinese Academy of Sciences, Beijing 100029, China*
[2]*Institute of Geology, Chinese Academy of Geological Sciences, Beijing 100037, China*
e-mail: yanzhen@mail.igcas.ac.cn

ABSTRACT: **The Qinling orogenic belt is one of world's great collisional orogenic belts, which extends from the Pamirs–West Kunlun to the Korean peninsula and occupies a key position in understanding of the evolution and assembly of Asia. This belt separates the North China and South China blocks. Extensive, thick Devonian clastic rocks, sandwiched between the Shangdan and Mianlue suture zones, are mainly infills of the Xicheng Basin and provide the principal sedimentary record of tectonism in the Qinling orogen. Devonian infills were subdivided into three subunits: the Upper Devonian Dacaotan Group, the Middle–Upper Devonian Shujiaba Group, and the Lower–Upper Devonian Xihanshui Group. Their provenance and tectonic setting are critical to understanding not only the tectonic evolution of Asia but also the global aspects of collisional regions. Compared with Devonian strata in the eastern part of the Qinling orogen, the Xicheng Basin was not seriously modified by Mesozoic tectonism.**

Petrologic studies demonstrate that the Dacaotan Group consists mainly of feldspathic litharenite with abundant volcanic fragments. In contrast, the Shujiaba and Xihanshui Groups contain more metamorphic and sedimentary fragments and fewer magmatics than other lithic fragments; these relations demonstrate that magmatic plutons were not extensively exposed at the time of deposition of these groups. On Q-F-L plots sandstones fall into the field of transitional arcs, but on Qm-P-K and Lm-Lv-Ls diagrams they plot in the fields of continental-arc and continental-suture rocks. The presence of volcanic lithic grains in the sandstones suggests they were derived mainly from a continental arc.

Major-element geochemistry of siltstones and mudstones demonstrate that most were derived from a continental arc, but some from an oceanic island arc. Trace-element geochemistry favors a continental-arc provenance mostly from felsic rocks. A high Cr content of siltstones and mudstones demonstrates that some mafic or ultramafic rocks were exposed in the source area and provided some detritus. Rare-earth-element patterns are very similar to those of sandstones in modern continental arcs. Devonian paleocurrent indictors demonstrate that this continental arc was located at the northern edge of the basin. This deduction demonstrates that the Qinling arc in the southern margin of the North China block was the major source of clastic debris in the Devonian Xicheng Basin; these relationships suggest that the sediments were most probably deposited in a forearc basin.

INTRODUCTION

The Qinling orogen occupies a key position in the Chinese part of the Central Asian Orogenic Belt, which extends from the Pamirs–West Kunlun to the Korean peninsula. It separates several northern Precambrian blocks (Tarim, Sino–Korean craton or North China block (NCB)) from southern blocks (such as the South China block (SCB)) (Fig. 1A) (Li et al. 1978; Mattauer et al. 1985; Zhang et al. 1989, 1995; Matte et al. 1996; Meng and Zhang 1999, 2000; Xiao et al. 2002a; Xiao et al. 2002b; Ratschbacher et al. 2003; Roger et al. 2003; Xiao et al. 2003; Schwab et al. 2004). Accordingly, the geology and tectonic evolution of the Qinling orogen are critical for a better understanding of the evolution and assembly of Asia.

A notable feature in this orogen is a thick, E–W striking Devonian marine and nonmarine clastic sequence (up to 4000 m thick) that is sandwiched between the Shangdan and Mianlue sutures (Fig. 1B). Although it is widely accepted that the orogen was finally consolidated in the early Mesozoic (Ames et al. 1993; Yin and Nie 1993; Hacker et al. 1998; Ye et al. 2000; Ratschbacher et al. 2003; Hacker et al. 2004), its Paleozoic history is much debated, and in particular the Devonian paleogeography. Mattauer et al. (1985) considered that the Devonian sediments were products of the first collision between the SCB and the NCB. Meng and Zhang (1999, 2000) suggested that deposition initially took place in the passive margin of the SCB. Hsü et al. (1987) suspected the Devonian age of these sediments, although no fossils were found from the flysch, and suggested that they represent a Triassic accretionary wedge on the active margin of the paleo-Tethys. Wang et al. (2002) systemically studied the tectonics of the Devonian sedimentary basins in the Qinling orogen and suggested that they formed in forearc regions during paleo-Qinling ocean subduction. Ratschbacher et al. (2003) and Hacker et al. (2004) recently suggested the Devonian deposits were incorporated into an accretionary wedge in a Devonian–Permian paleo-Tethys trench. Nevertheless, the provenance and tectonic setting of these sediments is still poorly known. New studies are required to reconcile differences between the Devonian age of the clastic rocks and the isotopic ages of ophiolites, paleomagnetic data, and the deformational and

 1527-1404/06/076-557/$03.00

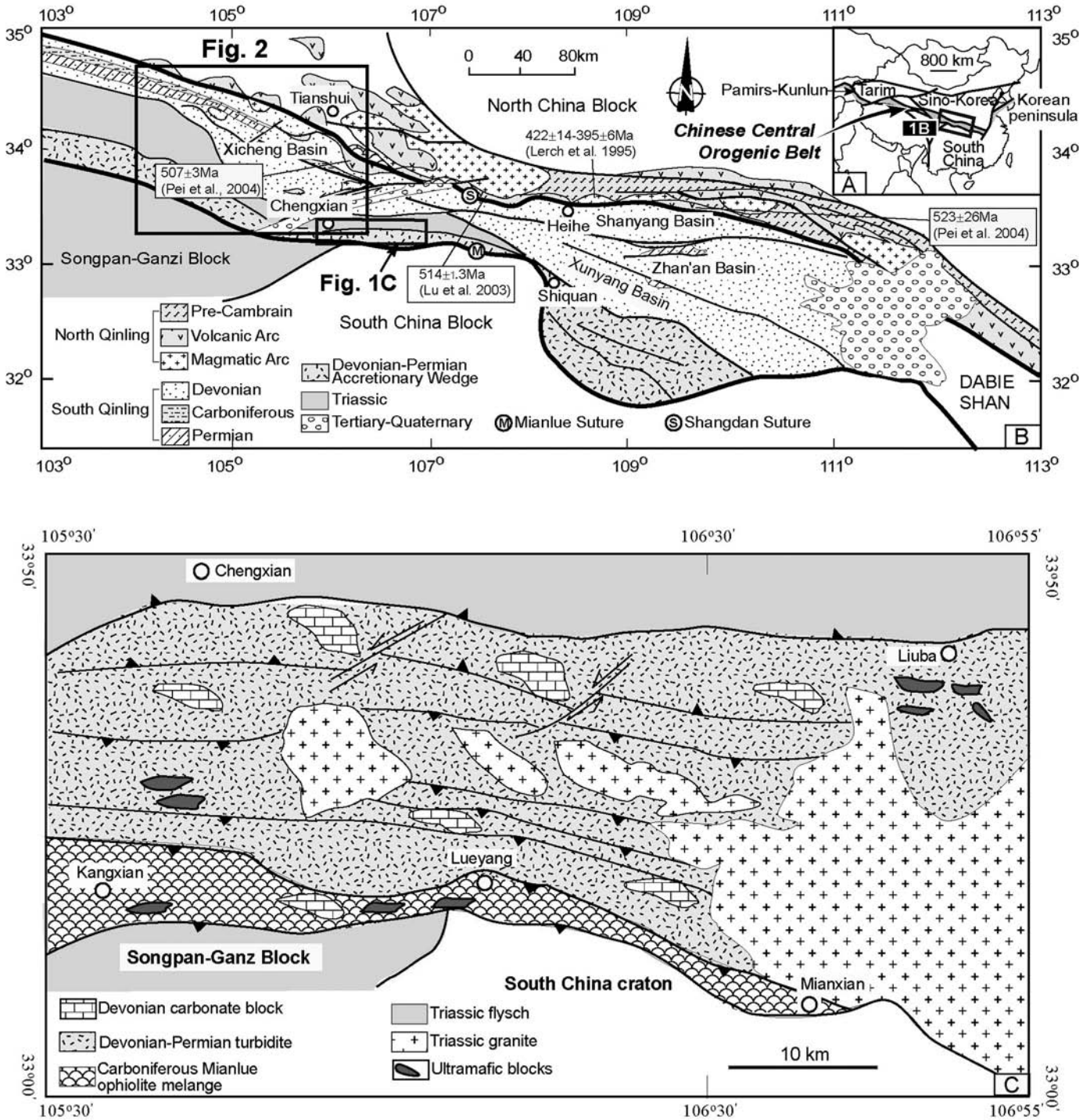

FIG. 1.—**A)** Tectonic framework of Chinese Central Orogenic Belt (Mattauer et al. 1985). **B)** Tectonic framework of the Qinling and location of the Devonian basins (Wang et al. 2002). **C)** Geological map of the Baishuijiang mélange (Wang 2003).

metamorphic history of the orogen, and a more reliable interpretation is required of the provenance and tectonic setting of the Devonian sediments in order to better understand the geodynamic framework of the Qinling orogenic belt and to reconstruct the Paleozoic evolution of the margins of the NCB and SCB within the evolution of this part of Eastern Asia.

The Xicheng Basin (Fig. 2A) is one of the biggest Devonian basins in the Qinling orogen and contains abundant Pb–Zn ore deposits. It is located on the southern margin of the Silurian–Devonian North Qinling arc (Lerch et al. 1995; Xue et al. 1996a, 1996b; Meng and Zhang 1999, 2000; Ratschbacher et al. 2003) in the western part of the Qinling and is spatially and temporally correlative with the evolution of the NCB and SCB. Basin fill consists of Early Devonian–Permian turbidites, and shallow-water and nonmarine sediments (Cao et al. 1990; Li et al. 1994; Fig. 2B), which can prove useful in discriminating detrital signatures of contrasting plate-tectonic settings. However systematic geological studies

of the provenance and tectonic setting of the Devonian rocks in the Xicheng Basin are rare.

In this paper, we focus on the detrital and geochemical composition of the Devonian sandstones in the Xicheng Basin in order to shed new light on their plate-tectonic setting and to provide firm evidence for understanding the Devonian paleogeography between the NCB and SCB.

Geological Setting

The Qinling orogen (Fig. 1B) contains early Paleozoic intra-oceanic island arcs and Silurian–Devonian magmatic arcs accreted to the southern margin of the NCB in the Silurian–Devonian (Mattauer et al. 1985; Yan 1985; Zhang et al. 1989; Lerch et al. 1995; Meng and Zhang 1999, 2000; Xue et al. 1996a, 1996b; Zhang et al. 1997; Ratschbacher et al. 2003). The Shangdan and Mianlue sutures separate the orogen into three main tectonic units (Zhang et al. 1995; Meng and Zhang 1999, 2000): North Qinling, South Qinling, and the northern marginal belt of the SCB. Recently, a Devonian–Permian accretionary wedge was defined along the northern margin of the SCB (Wang et al. 1999; Yang 1999; Wang et al. 2002; Wang 2003; Ratschbacher et al. 2003; Fig. 1B). Devonian sedimentation took place between the island arc and the accretionary wedge.

The North Qinling is adjacent to the southern margin of the NCB and comprises a lower Proterozoic Qinling complex (Qinling unit), two zones of early Paleozoic (~ 490–470 Ma) intra-oceanic-arc-type and backarc-type ophiolites (Danfeng and Heihe units), and a Devonian (~ 400 Ma) accreted magmatic arc (Shang and Yan 1988; Lerch et al. 1995; Sun et al. 1996; Xue et al. 1996a, 1996b; Xiao et al. 1999; Pei et al. 2005). The presence of these rocks demonstrates that this mid-Paleozoic orogen was associated with widespread Paleozoic magmatism and metamorphism. Hacker et al. (2004) interpreted the regional contact metamorphism in the North Qinling to be produced by 400 Ma magmatic arcs. Furthermore, Zhang et al. (1988) suggested that this belt was an early Paleozoic island arc. Ratschbacher et al. (2003) and Lerch et al. (1995) suggested that the North Qiling was a Late Silurian to Middle Devonian (422 ± 14 to 395 ± 6 Ma, Lerch et al. 1995; ~ 380 Ma, Shang and Yan 1988) Andean-type magmatic arc that formed by oblique northward subduction, imprinted on the deformed southern passive continental margin of the NCB. These studies demonstrate that the North Qinling contains remnants of an early Paleozoic island arc and a Devonian magmatic arc. Clastic sediments with abundant metamorphic detritus were deposited along the southern flank of the arc (Mattauer et al. 1985; Yu and Meng 1995; Meng et al. 1997).

In contrast, the South Qinling consists of a middle–upper Proterozoic low-grade-metamorphosed volcanic basement and a continuous sedimentary cover from the upper Proterozoic to the Middle Triassic. Ren et al. (1991) and Mattauer et al. (1985) suggested that Devonian and Silurian sedimentation took place on a passive margin. Meng and Zhang (1999, 2000), however, stated that the South Qinling was at the time in an extensional setting and served as the northern passive continental margin of the SCB in the middle Silurian–Devonian, and was rifted from the northern rim of the SCB in the Carboniferous–Permian. This suggests that the South Qinling should have begun to receive sediments from the North Qinling in the middle Paleozoic. According to geochemical data from Paleozoic clastic rocks, Gao et al. (1995) suggested that the SCB was accreted to the NCB along the Shangdan suture before the Carboniferous. In contrast, Ratschbacher et al. (2003) and Hacker et al. (2004) interpreted the South Qinling as a Silurian–Devonian accretionary wedge, and Wang (2003) suggested it was a Devonian–Permian mélange belt distributed along the northern margin of the SCB together with the Mianlue ophiolite (Fig. 1B).

In fact, in the Chengxian and Shiquan areas (Fig. 1C) a suite of turbidites with thin cherts, carbonates, and volcanic and pyroclastic rocks along the northern margin of the SCB was named the "Baishuijiang Group" and regarded as Silurian in age since the 1930s (Ye and Guan 1944). Volcanic blocks in the pyroclastic rocks include calc-alkaline basalt, basaltic dacite, andesite, andesitic tuff, and lava, and basalt blocks near Kangxian have yielded a zircon SHRIMP age of 812 ± 22 Ma (Wang 2003). *Cladopora palaeogracilis* Tchi, *Thamnopora* sp., *Paraortnograptus* sp., *Productus* sp., *Marginifera visceniana*, and small shelly fossils occur in some limestone blocks (B.M.G. Gansu 1982; B.M.G. Shaanxi 1994, 1999), demonstrating that they contain Cambrian, Ordovician, Devonian, and Carboniferous fauna. Wang (2003) found *Follicucullus* sp., *Albaillella* aff. Levis, *Srakaeopshaera* sp., *Albaillella excelsa* aff. Levis, *Follicucullus charveti*, *Pseudoalbaillella lomentaria*, *Albaillella* sp., *Albaillella triangularis*, *Follicucullus* sp., and *Radiolaria* sp. in thin-bedded limestone and chert. The geochemical character of the mudstone and sandstone matrix implies that they were derived from a continental arc (Wang 2003). The occurrence of different blocks with different ages and tectonic settings demonstrates that they belong to a mélange, and are juxtaposed against another Carboniferous–Permian Shiquan accretionary wedge (Fig. 1B; Wang et al. 1999; Wang et al. 2002) to the east. These rocks belong to the Silurian–Carboniferous Mianlue ophiolite mélange, located immediately south of the southern margin of the NCB.

Devonian rocks in the Qinling orogen are referred to as the Liuling Group in the eastern part of the orogen, and as the Shujiaba Group, the Xihanshui Group, and the Dacaotan Group in the western part. They overlie Paleozoic (Cambrian–Devonian) and Precambrian metavolcanic rocks with calc-alkaline geochemical signatures (Zhang et al. 1993; Liang 1994), and are sandwiched between the North Qinling arc and the Baishuijiang–Shiquan accretionary wedge.

Stratigraphy

The Xicheng Basin contains Devonian, Carboniferous, and Permian sediments (Fig. 2). Devonian rocks include the Lower–Upper Devonian Xihanshui Group, the Middle–Upper Devonian Shujiaba Group and the Upper Devonian Dacaotan Group (Regional Surveying Team of Shaanxi Province 1971). Carboniferous and Permian rocks crop out only in the center of the basin and are in fault contact with Devonian rocks (Fig. 2A). Carboniferous rocks are composed of turbidites at the base and conglomerate with coal intercalations at the top, reflecting a sedimentary evolution from deep-water fan to alluvial fan (Cao et al. 1990; Li et al. 1994). Permian strata consist of conglomerate, sandstone, radiolarian chert, and mudstone with *Neonereites–Protopaleodictyon*, which were deposited in a submarine-fan system (Wang et al. 1995). In the southern margin of the basin, Triassic calcareous siltstone, mudstone, and thin layers of limestone with *Lytophiceras* sp. may have formed as deep-water turbidites (Li et al. 1994). Finally, extensive Mesozoic granites with subduction-related calc-alkaline characteristics (Yan 1985; Huo and Li 1995) intruded these clastic rocks.

The Xihanshui Group in the southern part of the basin includes turbidite and reef blocks. The turbidites developed upwards into thin micrite and marl interbeds (Fig. 2B). Reef blocks with abundant Devonian coral fossils are in fault contact with the Devonian turbidites (Liu et al. 1992; Zhang et al. 1993; Huo and Li 1995; Li et al. 1994; Zhang et al. 1994) and overlie early Paleozoic metavolcanic rocks, schist, gneiss, and marble in the Wujiashan area (Fig. 2A). Early and Middle Devonian microfossils such as *Apiculiretusispora plicata*, *Acanthotriletes tenuispinosus*, and *Archaeozonotriletes variabilis* occur in turbidite siltstones (Li 1989), and Ordovician–Silurian *Leiofusa* aff. *Fusiformis*, *L.* cf. *puluitates*, *Synsphaeridium conglatinatum* Tim, *Leiopsophosphaera* sp. 1, *Trachysphaeridium* sp., and *Microhystridium* sp. occur in muddy schists (Zhang et al. 1999). Also, Zhang et al. (1999) obtained an Rb/Sr whole-rock age on greenschist-facies metavolcanic rocks of 1224.26 ± 28.99 Ma in the Wujiashan area. If these age data are reliable, we suggest that Proterozoic

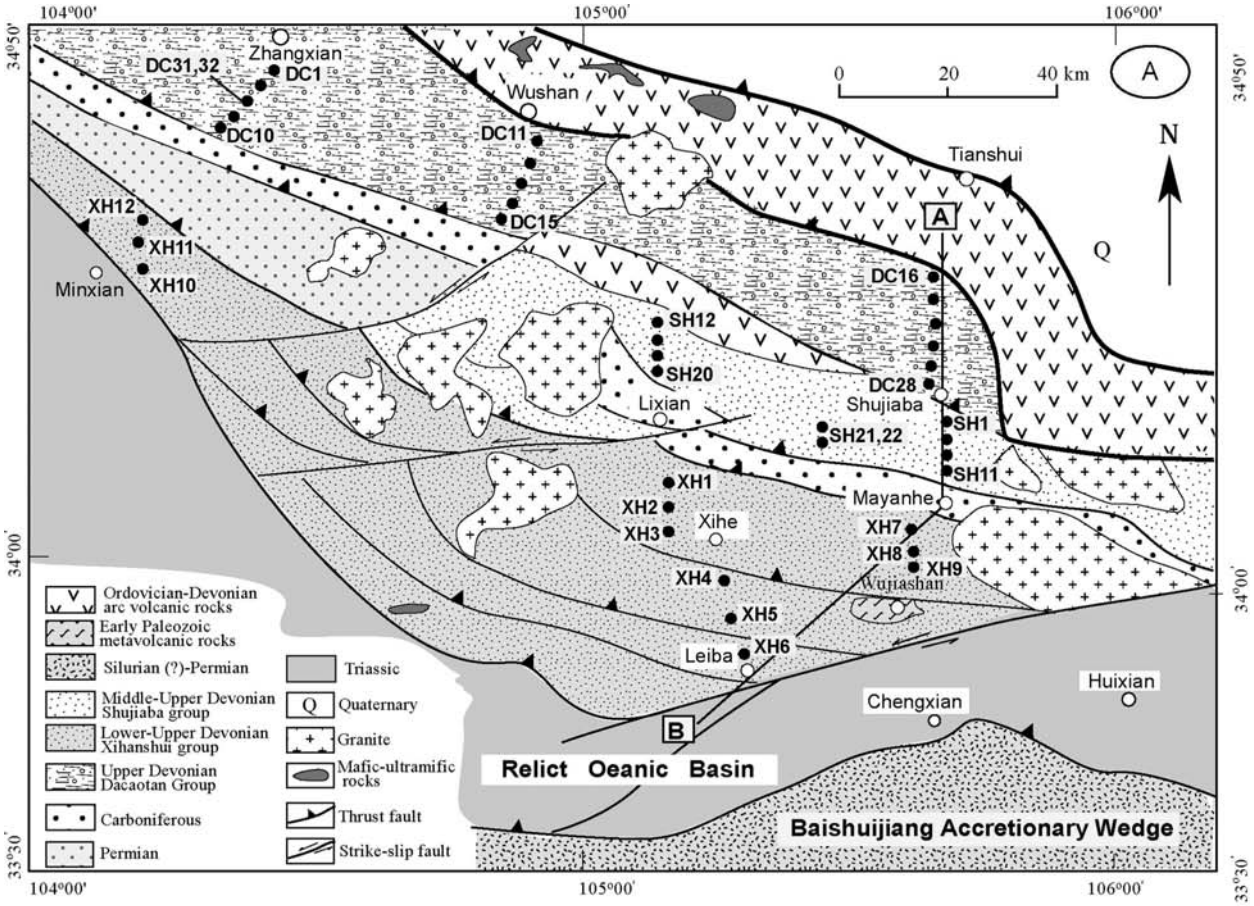
104°00'
105°00'
106°00'
34°50'
34°00'
33°30'
Zhangxian
DC31,32
DC1
DC10
Wushan
DC11
DC15
Tianshui
A
0 20 40 km
N
Q
XH12
XH11
XH10
Minxian
DC16
SH12
SH20
DC28
Shujiaba
Lixian
SH1
SH21,22
SH11
XH1
XH2
XH3
Xihe
Mayanhe
XH7
XH8
XH9
Wujiashan
XH4
XH5
XH6
Leiba
Huixian
Chengxian
B
Relict Oeanic Basin
Baishuijiang Accretionary Wedge
Ordovician-Devonian arc volcanic rocks
Early Paleozoic metavolcanic rocks
Silurian (?)-Permian
Middle-Upper Devonian Shujiaba group
Lower-Upper Devonian Xihanshui group
Upper Devonian Dacaotan Group
Carboniferous
Permian
Triassic
Quaternary
Granite
Mafic-ultramific rocks
Thrust fault
Strike-slip fault

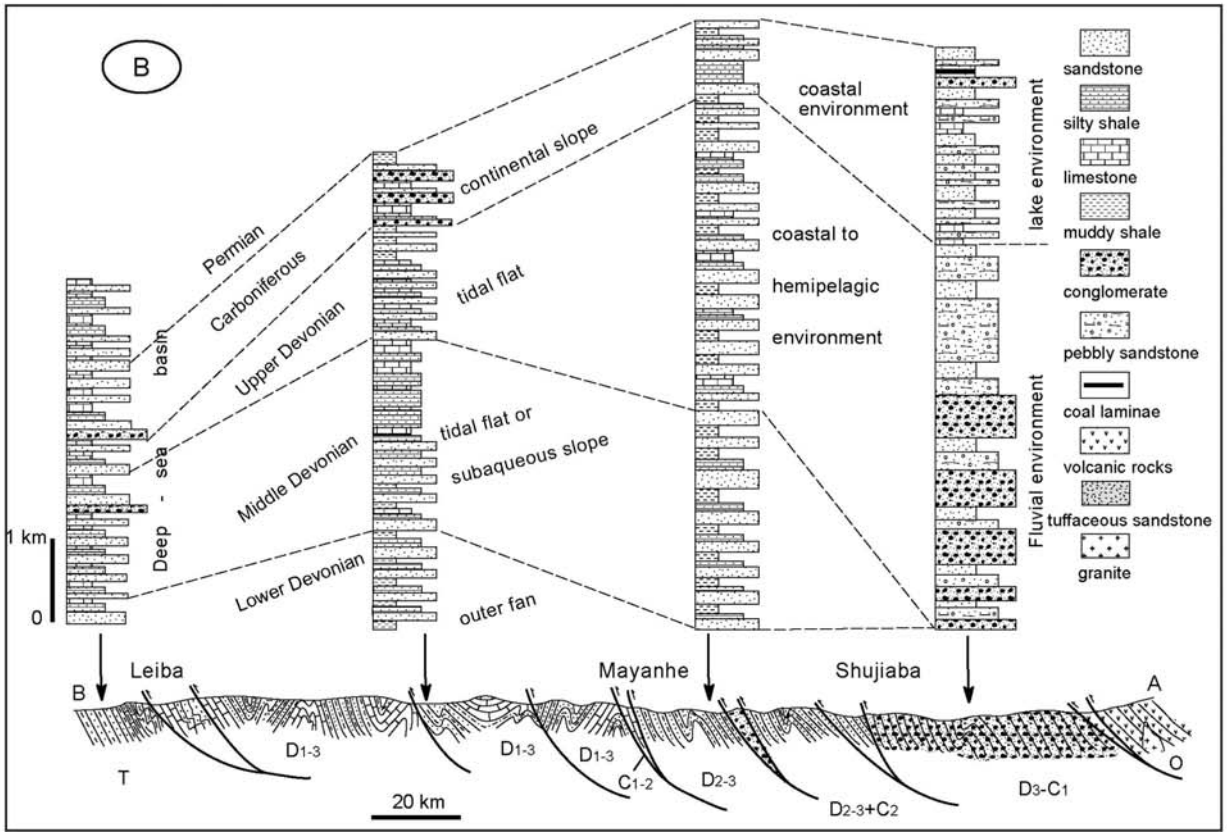
B
Permian
Carboniferous
Upper Devonian
Middle Devonian
Lower Devonian
basin
Deep - sea
1 km
0
continental slope
tidal flat
tidal flat or
subaqueous slope
outer fan
coastal environment
coastal to
hemipelagic
environment
lake environment
Fluvial environment
sandstone
silty shale
limestone
muddy shale
conglomerate
pebbly sandstone
coal laminae
volcanic rocks
tuffaceous sandstone
granite
Leiba
Mayanhe
Shujiaba
B
A
T
D1-3
D1-3
D1-3
C1-2
D2-3
D2-3+C2
D3-C1
O
20 km

rocks may constitute part of the basement of the Xihanshui Group, and the reef blocks are probably exotic.

The Shujiaba Group is exposed in the middle part of the Xicheng Basin (Fig. 2A), and was previously inferred to have a Middle Devonian age deduced from regional geological correlations (Ye 1986; Liu et al. 1992) and from fossils (Early to Late Devonian) in sandstones (Su and Huang 2000). However, its age has been redefined by the recent discovery of abundant Late Devonian spores in sandstones (Su and Huang 2000). Thick graywacke and thin layers of siltstone and mudstone contain grading and ripple cross-lamination in the lower part, and rhythmic thin layers of limestone and muddy siltstone contain a *Nereites* ichnofacies (Jin and Li 1997) in the upper part. The presence of thick turbidite packages and the absence of shallow-water deposits indicate a marine environment below wave base. Flute casts, cross-lamination, climbing ripples, graded bedding, and current-ripple lamination are consistent with deposition from turbidity currents.

The Dacaotan Group, exposed only in the northern part of the Xicheng basin, contains abundant Late Devonian plant fossils (e.g., *Leptophloeum rhombicum* Dawson; Regional Surveying Team of Shaanxi Province 1971), and is characterized by sandstones and lenticular conglomerates. The Dacaotan Group unconformably overlies the Danfeng unit of the North Qinling (Huo and Li 1995). Poorly organized, clast- and matrix-supported, and lenticular conglomerate beds are debris-flow deposits; imbricated clasts and low-angle cross-bedding indicate that this lithofacies was deposited mainly by streamflow processes (Yan et al. 2002). Some organized conglomerate lithofacies are highly comparable to gravel and coarse-grained sands deposited in braided streams under waning flow conditions by accretion of progressively smaller clasts in channels and longitudinal bars (Collinson 1986). Interbedded mudstones probably record stagnation and fluvial channel abandonment. Massive to planar-stratified and trough-cross-stratified sandstones that grade upward into ripple-laminated, fine-grained sandstones capped by thin mudstones is interpreted as streamflow deposits (Miall 1992). Paleocurrent data indicate that stream-dominated alluvial fans adjacent to the North Qinling along the northern basin margin transported sediment southwards (Du 1997).

TABLE 1.—*Counted and recalculated petrographic parameters of sandstones.*

Counted parameters:	
Qp = polycrystalline quartz grains	
Qm = monocrystalline quartz grains	
P = plagioclase feldspar grains	
K = potassium feldspar grains	
Lvf = volcanic lithic with felsic texture	
Lvmi = volcanic lithic with microlithic texture	
Lvl = volcanic lithic with lathwork texture	
Lvv = vitric volcanic lithic	
Lsa = argillite shale lithic	
Lsch = chert lithic	
Lsc = sedimentary carbonate lithic	
Lsi = siltstone lithic	
Lmv = metavolcanic lithic	
Lmm = polycrystalline mica lithic	
Lma = quartz-feldspar-mica aggregate lithic	
Lmp = phyllite lithic	
M = phyllosilicate minerals	
D = dense minerals	
Car = carbonate minerals	
Misc = miscellaneous and unidentified	
Q = total quartz grains	F = total feldspar grains
Lv = volcanic lithic grains	Ls = sedimentary lithic grains
Lm = metamorphic lithic grains	
Q = Qp + Qm	F = P + K
Lv = Lvf + Lvmi + Lvl + Lvv	Lvc = Lvf + Lvmi + Lvl
Lm = Lmv + Lmm + Lma + Lmp	
Ls = Lsa + Lsc + Lsch + Lsi	Lt = Lv + Ls + Lm + Misc
Recalcuted parameters:	
QtFL%Q = 100*Qt/(Qt + F + L)	QmPK%Q = 100*Qm/(Qm + P + K)
QtFL%F = 100*F/(Qt + F + L)	QmPK%P = 100*P/(Qm + P + K)
QtFL%L = 100*L/(Qt + F + L)	QmPK%K = 100*K/(Qm + P + K)
QmFLt%Qm = 100*Qm/(Qm + F + Lt)	
QtFL%F = 100*f/(Qt + F + L)	
QtFL%L = 100*L/(Qt + F + L)	
LmLvLs%Lm = 100*Lm/Lt	LvfLvmiLvi%Lvf = 100*Lvf/Lvc
LmLvLs%Lv = 100*Lv/Lt	LvfLvmiLvi%Lvmi = 100*Lvmi/Lvc
LmLvLs%Ls = 100*Ls/Lt	LvfLvmiLvi%Lvi = 100*Lvi/Lvc

METHODS

In order to define the source area of the basin, coarse-grained, unweathered, lithic sandstones were preferentially sampled to facilitate determination of lithic modes. From the ~ 250 Devonian sandstone samples collected, 48 of the most suitable (Fig. 2A) were point-counted following the Gazzi–Dickinson method. 500 points per section were counted and assigned to 22 categories (Table 1, Appendix 1). Criteria used for distinguishing lithic types, matrix types, and other components are those of Dickinson (1970) and Graham et al. (1976). Appendix 1 lists the raw point data, and Table 2 is the recalculated detrital modes that were plotted in Qt-F-L, Qm-F-Lt, Qm-P-K, and Lm-Lv-Ls diagrams. These parameters, explained in Table 1, were chosen to minimize redundancy and to lessen dependence on minor components.

Seventeen Devonian siltstone and mudstone samples were analyzed for major elements, trace elements, and rare earth elements (REEs) in the Key Laboratory of the Lithosphere, Institute of Geology and Geophysics, Chinese Academy of Sciences. Major-element concentrations were determined following standard X-ray fluorescence (XRF) techniques on an automatic Rigaku 3370 spectrometer. The REEs concentrations were determined by inductively coupled plasma mass spectrometry (ICP-MS) following conventional methods. For graphing purposes, the REE data were normalized to chondrite values following Taylor and McLennan (1985). The REE and trace-element distribution patterns (including La–Th–Sc relationships) were compared with the results of other studies conducted on provenance and crustal evolution (Taylor and McLennan 1985; McLennan 1989; McLennan et al. 1990).

RESULTS AND DISCUSSION

Sandstone Composition

48 sandstone samples in this study are feldspathic litharenite (mean $Qm_{23 \sim 25}F_{17 \sim 23}Lt_{52 \sim 60}$). They contain a large proportion of metamorphic (including metavolcanic and muscovite–quartz schist) fragments, attesting to a dominantly metamorphic provenance (Table 2). A majority of the samples are litharenite in which muscovite–quartz schist and sedimentary fragments are the dominant lithics. Despite the general similarity in sandstone composition in all of the samples, subtle and distinct changes in provenance throughout are distinguishable. The trends in framework-grain compositions are discussed below.

←

FIG. 2.—**A)** Geological map of the Xicheng Basin and location of samples; AB represents location of cross section. **B)** Cross section of the basin and columnar sections of Devonian rocks in the Xicheng Basin.

TABLE 2.—*Recalculated detrital modes for Devonian sandstones from the Xicheng Basin.*

Sample	Qt	F	L	Qm	F	Lt	Qm	P	K	Lm	Lv	Ls	Lvf	Lvmi	Lvl
DC1	25.8	20.5	53.8	19.7	20.5	59.8	49.0	33.8	17.2	55.1	24.9	20.0	7.6	75.8	16.7
DC2	30.7	20.9	48.4	23.6	20.9	55.5	53.0	32.9	14.2	47.5	23.9	28.6	3.5	78.9	17.5
DC3	28.8	30.6	40.6	20.0	30.6	49.4	39.5	39.5	20.9	55.7	14.8	29.6	6.7	76.7	16.7
DC4	34.4	15.4	50.2	24.6	15.4	60.0	61.5	27.0	11.5	51.8	23.9	24.3	1.7	73.3	25.0
DC5	32.5	16.7	50.8	23.5	16.7	59.8	58.5	29.0	12.5	51.0	20.2	28.9	10.9	71.7	17.4
DC6	35.2	17.4	47.5	25.7	17.4	57.0	59.6	22.5	17.8	52.8	23.8	23.4	14.3	73.2	12.5
DC7	26.8	25.2	48.0	22.2	25.2	52.6	46.8	39.5	13.7	52.5	24.6	22.9	12.3	70.2	17.5
DC8	23.3	37.6	39.2	18.4	37.6	44.1	32.8	46.0	21.2	58.9	22.4	18.8	17.9	48.7	33.3
DC9	33.0	16.7	50.3	26.6	16.7	56.7	61.4	21.4	17.1	43.4	36.1	20.5	11.8	77.6	10.6
DC10	23.9	20.5	55.5	19.1	20.5	60.4	48.2	38.6	13.2	46.4	25.7	27.9	15.4	61.5	23.1
DC11	40.4	11.1	48.5	26.9	11.1	62.0	70.7	20.7	8.5	46.3	31.3	22.5	10.7	56.0	33.3
DC12	25.1	19.1	55.8	20.2	19.1	60.7	51.3	33.0	15.7	43.9	35.8	20.3	9.7	60.2	30.1
DC13	42.9	22.2	34.9	28.0	22.2	49.8	55.7	32.9	11.4	55.6	22.2	22.2	15.6	78.1	6.3
DC14	29.7	10.8	59.6	18.9	10.8	70.3	63.7	21.9	14.4	45.4	30.4	24.2	6.9	81.6	11.5
DC15	35.4	20.0	44.6	25.6	20.0	54.4	56.1	29.1	14.8	47.7	24.3	28.0	13.2	83.0	3.8
DC16	40.4	20.1	39.5	28.3	20.1	51.6	58.5	27.1	14.4	54.4	36.8	8.8	4.3	92.9	2.9
DC17	31.7	29.7	38.6	23.2	29.7	47.1	43.9	33.2	22.9	35.1	34.6	30.4	3.2	82.5	14.3
DC18	21.8	17.5	60.7	14.5	17.5	67.9	45.3	28.9	25.8	44.2	35.9	19.9	13.9	67.3	18.8
DC19	34.5	12.8	52.7	22.7	12.8	64.5	64.0	21.7	14.3	43.1	35.0	21.9	12.7	81.0	6.3
DC20	26.7	22.4	50.9	18.8	22.4	58.7	45.6	33.5	20.9	44.5	34.6	20.9	15.9	72.7	11.4
DC21	34.5	20.3	45.2	24.9	20.3	54.8	55.2	28.3	16.6	53.8	26.0	20.2	5.3	75.4	19.3
DC22	34.0	19.7	46.3	24.1	19.7	56.1	55.0	26.6	18.3	42.2	30.4	27.4	17.2	78.1	4.7
DC23	29.4	22.0	48.6	21.6	22.0	56.4	49.5	32.6	17.9	55.1	23.0	21.8	5.4	83.9	10.7
DC24	39.8	19.1	41.2	28.8	19.1	52.1	60.2	23.7	16.1	53.7	30.5	15.8	3.2	79.0	17.7
DC25	39.7	21.0	39.3	30.1	21.0	48.9	58.8	25.9	15.3	54.6	25.5	19.9	0.0	76.0	24.0
DC26	35.3	18.2	46.5	27.5	18.2	54.3	60.1	25.9	14.0	51.3	27.6	21.1	9.4	75.0	15.6
DC27	32.6	20.6	46.8	25.4	20.6	54.0	55.2	29.1	15.7	53.8	18.4	27.8	0.0	83.7	16.3
DC28	34.5	18.2	47.3	27.1	18.2	54.7	59.8	26.3	13.8	55.6	29.1	15.4	6.1	71.2	22.7
STDEV	5.6	5.6	6.4	3.8	5.6	6.0	8.3	6.2	3.7	5.7	5.9	4.9	5.3	9.2	8.2
AVERAGE	32.2	20.2	47.5	23.6	20.2	56.2	54.3	29.7	16.1	49.8	27.6	22.6	9.1	74.5	16.4
SH1	7.3	27.9	42.3	24.3	27.9	47.8	46.5	41.9	11.6	54.5	38.8	6.7	9.9	59.3	30.9
SH2	30.0	25.1	44.9	22.4	25.1	52.5	47.2	36.8	16.0	53.2	19.7	27.1	9.3	67.4	23.3
SH3	34.4	28.6	37.0	22.5	28.6	48.9	44.1	30.7	25.2	57.1	13.6	29.3	0.0	91.3	8.7
SH4	38.1	18.6	43.3	24.1	18.6	57.3	56.4	29.9	13.7	57.5	15.9	26.6	11.8	32.4	55.9
SH5	31.8	20.3	47.9	20.5	20.3	59.2	50.2	32.5	17.2	75.6	8.0	16.4	10.5	47.4	42.1
SH6	34.4	14.1	51.5	26.5	14.1	59.5	65.3	29.1	5.5	66.4	9.5	24.1	8.3	79.2	12.5
SH7	30.3	26.2	43.5	24.4	26.2	49.4	48.2	36.1	15.7	74.8	9.3	15.9	15.0	65.0	20.0
SH8	35.8	19.8	44.4	28.5	19.8	51.7	59.1	26.6	14.3	62.4	19.7	17.9	4.7	53.5	41.9
SH9	32.6	22.5	44.9	26.7	22.5	50.8	54.3	24.3	21.4	71.2	10.8	18.0	12.5	50.0	37.5
SH10	28.8	37.7	33.5	24.6	37.7	37.7	39.5	44.0	16.5	72.3	17.5	10.2	6.9	65.5	27.6
SH11	32.0	23.7	44.2	24.1	23.7	52.1	50.4	26.3	23.3	63.3	10.1	26.6	0.0	45.5	54.5
SH12	37.9	16.0	46.1	26.5	16.0	57.5	62.3	22.6	15.1	63.9	10.0	26.1	4.3	56.5	39.1
SH13	28.1	20.7	51.2	24.9	20.7	54.4	54.6	23.8	21.6	59.2	20.8	20.0	0.0	69.8	30.2
SH14	36.0	23.5	40.4	26.8	23.5	49.7	53.2	24.4	22.4	60.7	21.9	17.4	11.4	65.9	22.7
STDEV	7.6	5.9	4.8	2.1	5.9	5.7	7.1	6.8	5.3	7.4	8.1	6.8	5.0	14.9	14.2
AVERAGE	32.9	23.2	43.9	24.8	23.2	52.0	52.2	30.6	17.1	63.7	16.1	20.2	7.5	60.6	31.9
XH1	33.5	15.3	51.2	24.0	15.3	60.7	61.0	25.1	13.8	58.7	34.3	7.1	4.6	78.2	17.2
XH2	29.7	13.6	56.7	21.2	13.6	65.2	60.9	23.1	16.0	54.2	19.3	26.5	10.0	80.0	10.0
XH3	33.5	11.7	54.7	23.6	11.7	64.6	66.9	19.4	13.7	52.8	21.8	25.5	11.9	83.1	5.1
XH4	34.8	20.0	45.1	25.7	20.0	54.3	56.2	28.3	15.5	48.0	25.6	26.5	31.4	60.8	7.8
XH5	30.5	18.7	50.8	22.4	18.7	58.9	54.5	29.3	16.2	51.0	32.7	16.3	31.7	47.6	20.6
XH6	29.5	22.1	48.4	19.9	22.1	58.0	47.4	33.5	19.1	51.9	30.3	17.8	11.5	67.2	21.3
STDEV	7.5	6.3	9.9	5.1	6.3	11.3	11.7	7.5	4.5	12.5	8.8	6.4	6.6	16.8	12.2
AVERAGE	31.9	16.9	51.2	22.8	16.9	60.3	57.8	26.5	15.7	52.7	27.3	20.0	16.8	69.5	13.7

Quartz and Feldspar Mineral Grains.—Quartzose grains remain relatively constant types in the studied samples. Their types are monocrystalline (Qm) and polycrystalline (Qp) with evident scaly inclusions and undulatory extinction, which suggests these quartz grains originated from a metamorphic region. The presence of monocrystalline quartz (inclusionless and with uniform extinction) and potassium feldspar suggests a partial felsic volcanic or shallow intrusive source component (Fig. 3C). Clear, inclusion-free grains, and embayment textures suggestive of a volcanic origin, are most common in monocrystalline quartz. The presence of elongate polycrystalline quartz grains with preferred orientation suggests derivation from metamorphic rocks. Feldspar grains are subangular and not strongly altered (Fig. 3C, F).

Lithic Fragments.—The relative average percentage of various lithic fragment types shows the most dramatic changes in the three units (Table 2). Although metamorphic fragments (Fig. 3) dominate in Devonian sandstone samples, a pronounced characteristic of the other lithic fragments is the abundance of volcanic fragments in the Dacaotan Group sandstones. These volcanic fragments are microlitic and fine-grained felsic fragments with minor lathwork textures (Fig. 3A). Meta-

morphic fragments contain polycrystalline quartz (Fig. 3B, E), metamorphic mica and quartz in variable proportions (Fig. 3F), fine-grained mica and quartz, and chlorite aggregates (Fig. 3D). Planar fabric is their character. Sedimentary fragments include chert (ch) and argillite-shale (Ls). The former show microcrystalline but monomineralic silica aggregates (Fig. 3D); the latter are murky fine-grained argillaceous fragments with occasional enclosed detrital silt clasts (Fig. 3D). Some aggregate quartz fragments show intergrown crystalline quartz without a significant planar fabric (Fig. 3E, left corner).

The polycrystalline mica, quartz–mica tectonite, and foliated metaquartzite fragments form a continuum of related metamorphic types that are mainly metasedimentary. Similarly, distinguishing unmetamorphosed argillite-shale from metamorphic quartz–mica tectonite is difficult, and at times arbitrary. Also, foliated metaquartzite, chert, and aggregate quartz, consisting of fine-grained vein, nonfoliated quartzite, and other nonfoliated quartz aggregates, are textural variants of polycrystalline quartz grains that are operationally difficult to differentiate with consistency.

Dense and Micaceous Minerals.—Dense minerals are less 1% and observed in some thin sections. Zircon and pyrite are common in some litharenite samples, and one pyroxene grain occurs in a thin section. Titanite also occurs in some samples. Micaceous grains consist of muscovite and sericite crystals. Muscovite shows elongate, oriented grains, indicating derivation from a metamorphic source; sericite shows numerous fine-grained grains, which possibly were formed by diagenesis, metamorphism, or other alteration processes.

Sandstone Detrital Modes

The framework mineral composition of sandstone samples from the Devonian sedimentary rocks (Table 2; Fig. 3) indicates that lithic fragments are dominant, but quartz and feldspar grains are subequal. Metamorphic and sedimentary rock fragments are more common than volcanic rock fragments, as shown by the site mean distributions in Figure 4. These different lithic types in the sandstone samples suggest that volcanic, metamorphic, and sedimentary rocks were exposed in the source area, and metamorphic rocks dominated the hinterland (Fig. 3D).

Figure 4A is a Qt-F-L diagram that clearly shows the low quartzose, high lithic content and subequal amounts of quartz and feldspar of the Devonian rocks. Figure 4B, a Qm-F-Lt plot, demonstrates the effect of including Qp in Lt rather than Q, and again emphasizes the less quartzose nature of the Devonian rocks. All sandstone samples fall within the fields of transitional and dissected arc settings, indicating that a magmatic arc was the predominant source area for the Devonian sandstones. Some sandstone samples from the Dacaotan and the Xihanshui groups fall within the field of a recycled orogen including foreland uplift, collision orogen, and accretionary prism (Dickinson and Suczek 1979), which suggests that some detritus was derived from a collision orogen or an accretionary prism (Fig. 4B).

Marsaglia and Ingersoll (1992) studied sandstone and sand petrographic compositional data collected from intraoceanic arc, remnant arc, continental arc, strike-slip continental arc, and triple junction tectonic settings. Intraoceanic-arc and remnant-intraoceanic arc provenances are two subunits of the undissected arc defined by Dickinson and Suczek (1979). The strike-slip-continental-arc category refers to continental-arc systems affected by periods of intra-arc or fore-arc strike-slip movement or oblique subduction; triple-junction arc provenance refers to sources at plate triple junctions involving at least one subduction zone, where arc systems are perturbed due to collision events or transitional tectonic settings (Marsaglia and Ingersoll 1992). The tectonic transformation involved with strike-slip-continental-arc and triple-junction provenances may result in uplift and erosion of forearc, arc, and backarc sequences, producing sands with distinctively different compositions. With increased dissection and erosion, the batholithic core of the arc is gradually exposed and initially produces sand with a transitional-arc provenance (Dickinson 1982; Dickinson and Suczek 1979). Marsaglia (1992) suggested that a transitional-arc provenance could also be produced in arc triple-junction settings, and the triple-junction Qt-F-L means occurred predominantly within the transitional-arc field, whereas the strike-slip-continental Qt-F-L means occurred primarily in the dissected-arc field. More quartzose, metamorphic and sedimentary fragments, and minor volcanic fragments are characteristic of sandstones derived from a continental arc (Marsaglia and Ingersoll 1992). These characteristics indicate that the lithic fragments of the sands and sandstones can provide reliable information on provenance settings. Although the Devonian sandstones fall within the provenance field of transitional arc, as shown by site-mean distributions in Figure 4A and B, metamorphic and sedimentary fragments are the major lithic detritus. This indicates that the Devonian sandstones were probably derived from triple junctions or continental arcs.

Figure 4C, a Qm-P-K plot, shows the relative proportions of quartz and feldspar grains derived mainly from granitic rocks with contributions of variable amount from volcanic and metamorphic rocks. Dickinson and Suczek (1979) defined a curve that becomes more quartz-rich with an increasing ratio of plutonic to volcanic components in magmatic-arc provenances. The quartz may result from a combination of more felsic magmatism, increased unroofing of plutonic roots of the arc, and enhanced rates of weathering/transport in continental arcs due to their greater subaerial extent relative to largely submerged intraoceanic arcs (Marsaglia and Ingersoll 1992). All sandstone samples from circum-Pacific subduction complexes fall between the dashed lines representing 33% and 50% quartz (Qm), and the mean ratios of total feldspar to quartz are uniformly between 1:1 and 2:1 (Dickinson 1982). Additionally, these sandstone samples from other forearc basins also fall within the same field, but also include more quartzose compositions which extend toward the dashed line at 67% Qm, representing a quartz-to-total-feldspar ratio of 2:1. The Xicheng Devonian sandstones, however, fall between the dashed lines representing 33% and 67% Qm (Fig. 4C), which suggests that these Devonian rocks were produced by extensive sedimentary reworking of arc-derived detritus within a forearc region. It is interesting to note that the proportion of K-feldspar does not vary significantly from the Xihanshui Group to the Dacaotan Group, indicating that the continental-arc provenance was not exhumed deeply enough to expose its plutonic root.

Figure 5A, a LmLvLs plot, clearly shows that the Devonian sandstone samples cluster near the Lm corner but overlap within the accretionary prism and suture belts of provenance fields, which suggests that these sandstones were deposited in a forearc region and were derived from metamorphic envelopes of the accretionary prism and suture zones associated with an arc. Ingersoll and Suczek (1979) found that sandstones derived from magmatic arcs, accretionary prisms, suture belts, and rifted continental margins can be differentiated readily using lithic detritus. As well, they were able to recognize virtually separate fields for forearc and backarc depositional sites in the Lm-Lv-Ls plot, whereas the higher Lm values in forearcs reported by Ingersoll and Suczek (1979) result from the erosion of metamorphic envelopes associated with the plutonic roots of an arc.

In order to define the type of volcanic-rock provenance, Marsaglia (1991, 1992) discussed the importance of microcrystalline volcanic lithic textures. Microcrystalline volcanic lithic proportions for arc-related sands indicate an overall dominance of microlitic textures and a maximum felsic component of 40% Lvf; continental arcs show a wide range of values, but strike-slip-continental-arc sands have felsic percentages greater than 5%; triple-junctions sands are bimodal, with one group showing anomalously low microlitic percentages, and the other, a high microlitic content

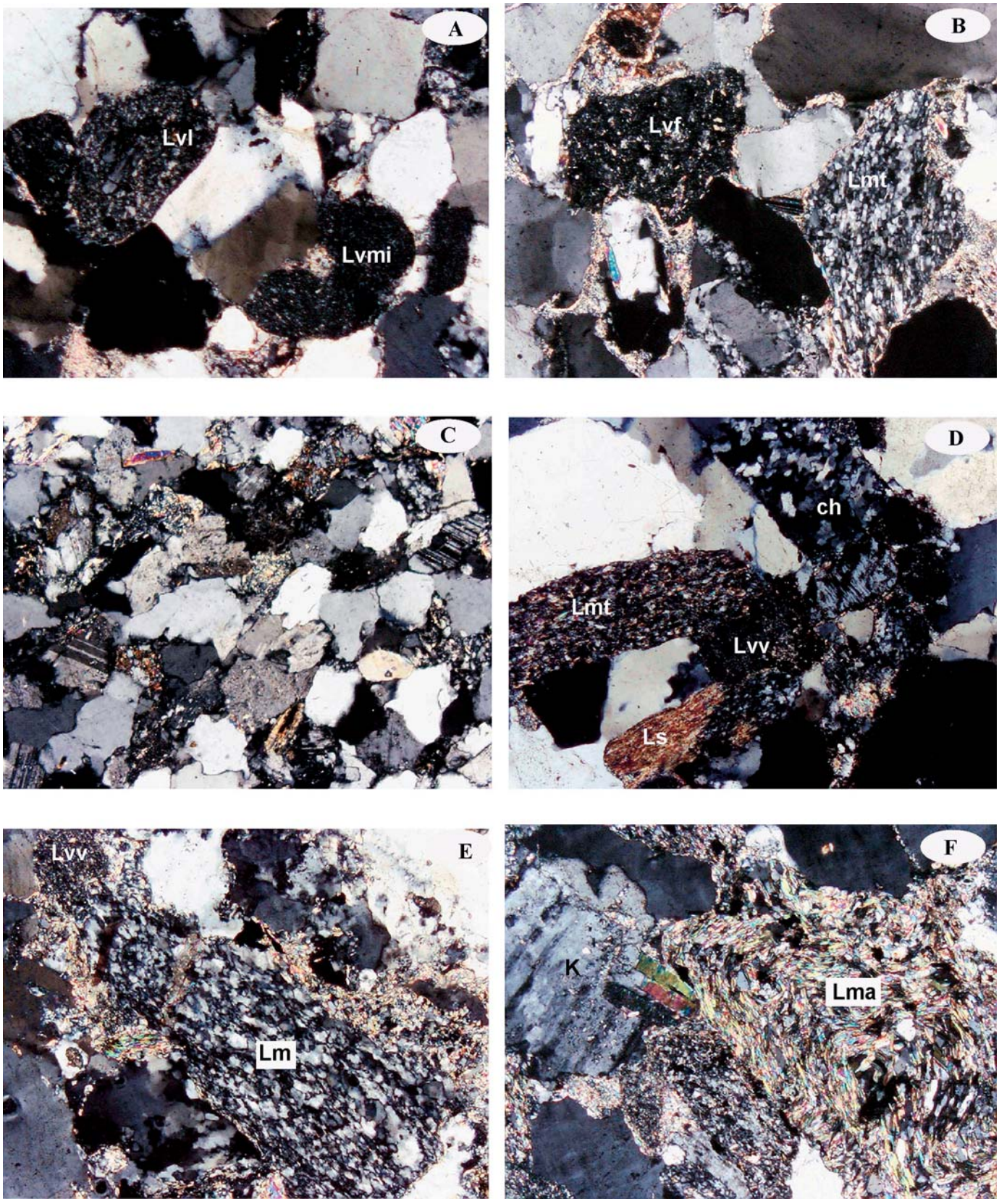

FIG. 3.—Photomicrographs with cross-polarized light of grain types as important source-rock indicators of Devonian sandstone in the Xicheng Basin (field of view, 3.1 mm). **A)** Volcanic fragment with lathwork (Lvl) and microlitic (Lvmi) textures in the Dacaotan Group sandstone. **B)** Volcanic fragments with felsic texture (Lvf) and foliated metaquartzites with a planar fabric (Lmt) in the Dacaotan Group sandstone. **C)** Abundant feldspar grains and monocrystalline quartz grain with embayment

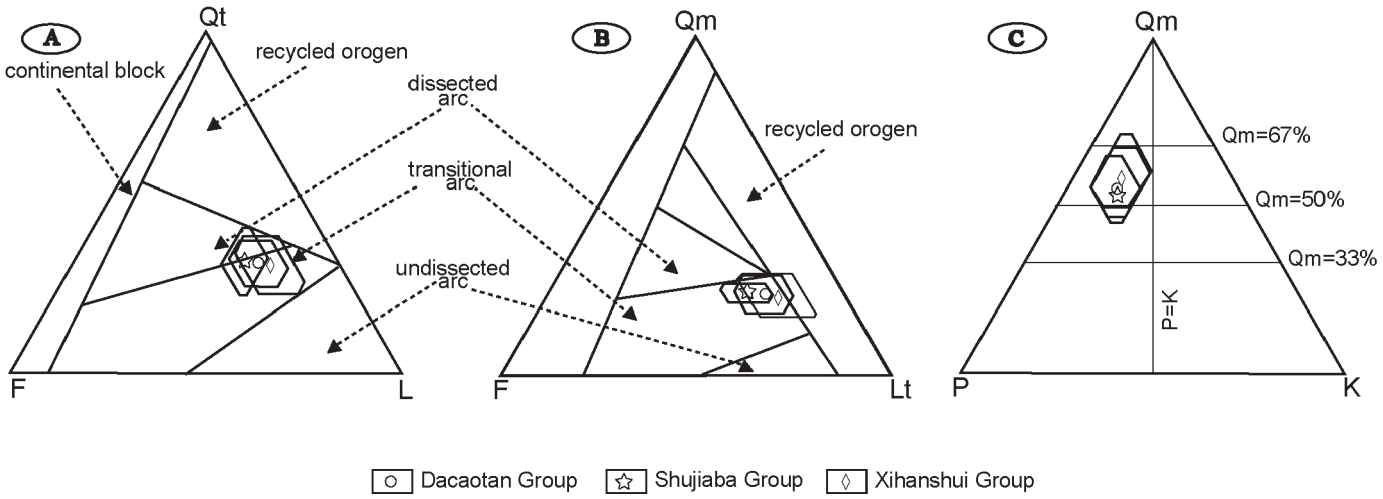

FIG. 4.—**A)** Qt-F-L, **B)** Qm-F-Lt, and **C)** Qm-P-K ternary diagrams of sandstone samples of the Xicheng Basin infill (after Dickinson 1985; Ingersoll and Suczek 1979); Qt, Qm, F, P, K, L, and Lt indicate total quartz, monocrystalline quartz, total feldspars, plagioclase, potassium feldspar, lithoclasts, and total lithoclasts including polycrystalline quartz grain, respectively.

(Marsaglia and Ingersoll 1992). All of the sandstone samples fall within the mixed field on a Lvf-Lvmi-Lvl plot, indicating that their volcanic detritus was more likely derived from a continental arc rather than an oceanic arc (Fig. 5B).

Siltstone and Mudstone Geochemical Data

The geochemical analysis of sedimentary rocks is a valuable tool for provenance studies of matrix-rich sandstones as long as the bulk composition is not strongly affected by diagenesis, metamorphism, or other alteration processes (McLennan et al. 1993). Sedimentary rocks in different tectonic settings have distinctive geochemical characteristics. The geochemical composition of sedimentary rocks can help to identify minor constituents that might be integral to tectonic interpretations (e.g., magmatic arc, ophiolitic compositions; McLennan 1989). Discrimination of tectonic settings on the basis of major element data was also proposed by Bhatia (1983), which includes oceanic island arc, continental arc, active continental margin, and passive margin.

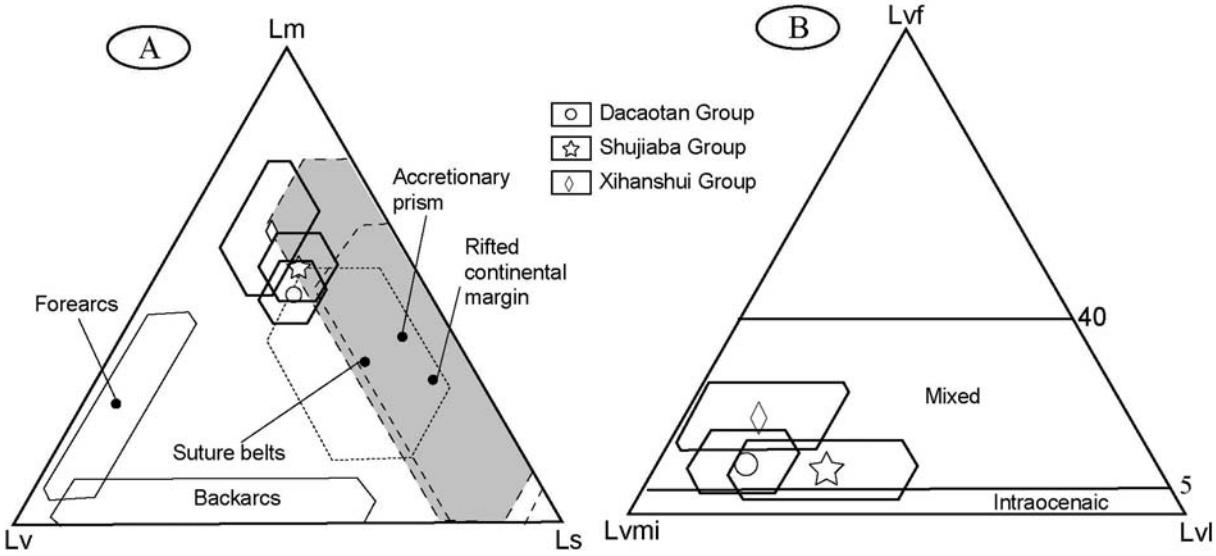

FIG. 5.—**A)** Lm-Lv-Ls and **B)** Lvf-Lvmi-Lvl ternary diagrams of sandstone samples of the Xicheng Basin fill (after Marsaglia and Ingersoll 1992); Lm, Lv, and Ls indicate metamorphic, volcanic, sedimentary fragments, respectively; Lvf, Lvmi, and Lvl indicate volcanic lithic with felsic texture, microlitic, and lathwork texture, respectively.

←

textures in the Shujiaba Group sandstone. **D)** Quartz–mica schist fragment with planar texture (Lmt), argillaceous fragment (Ls), vitric volcanic fragment (Lvv), and chert fragment (ch) in the Shujiaba Group sandstone. **E)** Quartz–schist fragment (Lm), vitric volcanic fragment (Lvv), and intergrown crystalline quartz in the Xihanshui Group sandstone. **F)** Quartz–feldspar–mica aggregate fragment (Lma) with planar texture and microcline grain (K) in the Xihanshui Group sandstone.

TABLE 3.—*Major-element concentrations in weight percent (wt.%) for Devonian siltstones and mudstones.*

Sample	Na_2O	MgO	Al_2O_3	SiO_2	P_2O_5	K_2O	CaO	TiO_2	MnO	Fe_2O_3	FeO	Total	K_2O/Al_2O_3	K_2O/Na_2O
DC29	0.12	2.8	17.62	59.4	0.16	5.02	0.96	0.84	0.12	5.95	1.26	94.25	0.28	1.79
DC30	0.95	5.52	18.31	58.14	0.09	5.49	3.51	1.42	0.05	1.62	4.48	99.58	0.30	0.99
DC31	1.5	2.6	17.32	59.76	0.09	3.78	3.45	0.47	0.02	0.52	4.63	94.14	0.22	1.45
SH15	0.32	1.5	20.73	61.21	0.12	5.23	<0.01	0.82	0.02	2.98	2.17	95.1	0.25	3.49
SH16	0.25	1.68	20.08	61.7	0.14	5.49	<0.01	0.85	0.02	3.33	1.63	95.17	0.27	3.27
SH17	1.27	3.5	18.77	59.75	0.14	4.09	<0.01	0.82	0.05	1.89	4.53	94.81	0.22	1.17
SH18	1.38	3.64	19.12	59.41	0.14	4.03	<0.01	0.82	0.05	1.98	4.68	95.25	0.21	1.11
SH19	1.3	2.65	17.73	59.01	0.11	3.91	2.3	0.77	0.04	2.54	4.4	94.76	0.22	1.48
SH20	0.7	2.47	20.04	59.62	0.1	4.72	0.44	0.84	0.04	2.83	4.22	96.02	0.24	1.91
SH21	0.8	2.53	20.34	58.92	0.11	4.43	0.58	0.81	0.04	2.31	4.67	95.54	0.22	1.75
SH22	0.82	2.4	16.88	60.06	0.18	6.7	2.46	0.84	0.05	1.2	4.42	96.01	0.40	2.79
XH7	2.72	3.51	12.15	59.7	0.14	3.24	6.18	0.64	0.09	1.37	3.3	93.04	0.27	0.92
XH8	0.85	3.56	12	47.44	0.12	2.47	13.68	0.54	0.07	1.01	3.38	85.12	0.21	0.69
XH9	1.23	3.62	17.71	56.58	0.14	4.16	0.28	0.73	0.04	1.52	4.42	90.43	0.23	1.15
XH10	1.44	3.37	18.1	60.59	0.14	3.53	0.27	0.78	0.06	1.71	5.07	95.06	0.20	1.05
XH11	2	3.62	19.12	59.16	0.14	3.85	0.44	0.78	0.04	2.03	4.51	95.69	0.20	1.06
XH12	0.82	2.99	11.89	53.02	0.12	2.54	11.11	0.56	0.09	0.96	3.24	87.34	0.21	0.85

Major-Element Geochemistry.—The major-element compositions of all Devonian siltstones and mudstones are shown in Table 3. A slight enrichment of SiO_2 (wt. %) content in siltstones, as compared to mudstones, can be attributed to the variation of quartz in these rocks. The Na_2O content for the siltstones is different. The depletion of Na_2O (< 1%) in the rocks (Table 3) can be attributed to a smaller amount of Na-rich plagioclase, consistent with the petrographic data. K_2O and Na_2O contents and their ratios are also consistent with the petrographic observations, according to which plagioclase feldspar dominates over K-feldspar. Al_2O_3 content is high in the siltstones but decreases in the mudstones. Generally low concentration of Fe_2O_3 and TiO_2 in the Devonian samples reflects low abundances of heavy minerals such as Ti-bearing biotite, ilmenite, titanite, and titaniferous magnetite in the analyzed samples. K_2O/Al_2O_3 ratios in all analyzed samples are less than 0.2, indicating that most K_2O is present in feldspar.

All the analyzed samples of the Shujiaba Group fall in the oceanic-island-arc field of the TiO_2 versus $Fe_2O_3{}^T$ + MgO plot (Fig. 6A), but some samples of the Xihanshui and Dacaotan Groups plot in the continental arc field. In the Al_2O_3/SiO_2 versus $Fe_2O_3{}^T$ + MgO diagram (Fig. 6B), all samples fall in the oceanic-island-arc field except for two samples of the Xihanshui Group. High Al_2O_3/SiO_2 ratios are an indication of quartz depletion in the Devonian sandstones. These discrimination diagrams suggest that the tectonic setting of the Xicheng Basin in which Devonian sandstones were deposited was that of an island arc.

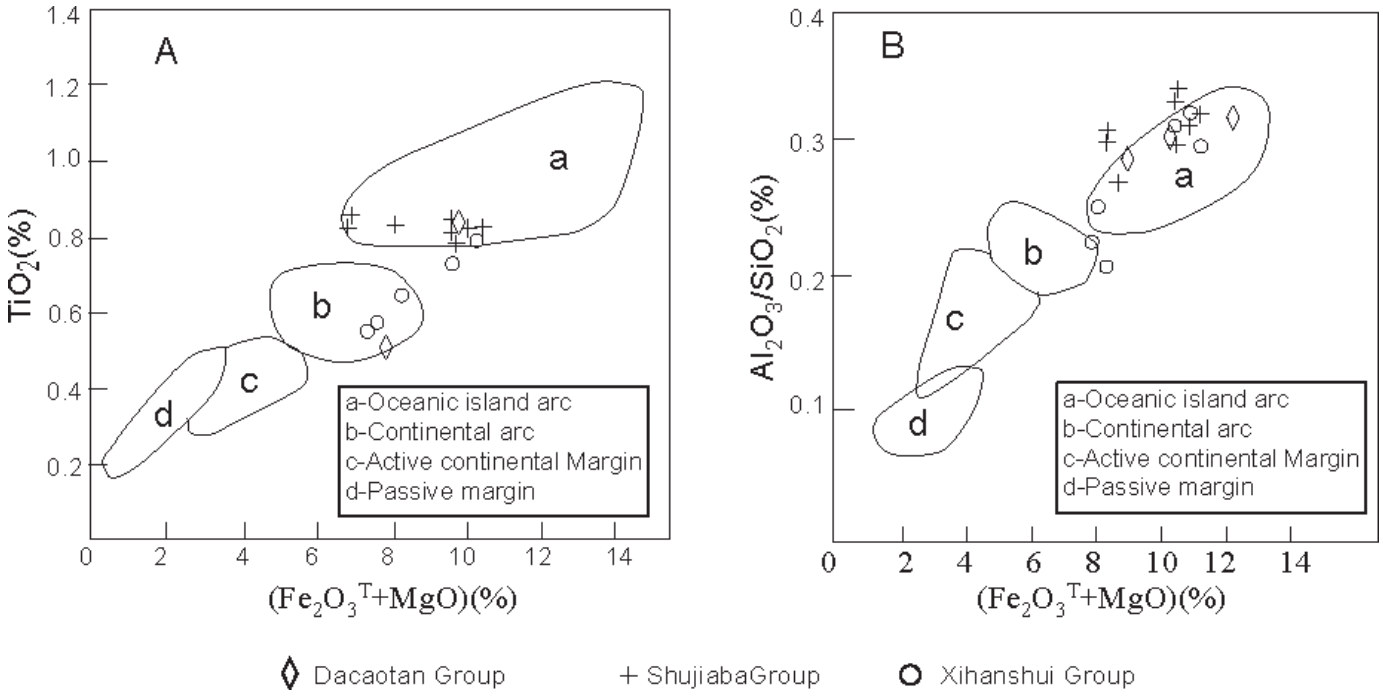

FIG. 6.—Tectonic setting discrimination diagrams for the Devonian siltstones and mudstones (after Bhatia 1983). **A)** TiO_2–$Fe_2O_3{}^T$ + MgO; **B)** Al_2O_3/SiO_2–$Fe_2O_3{}^T$ + MgO.

TABLE 4.—*Trace elements in ppm for Devonian siltstones and mudstones.*

Sample	DC29	SH15	SH16	SH17	SH18	SH19	SH20	SH21	SH22	XH7	XH8	XH9	XH10	XH11	XH12
Sc	17.4	19.5	21.4	18.2	19.4	15	17	13	19	14	13	17	19	16	14
V	115	132	141	118	124	143	156	167	139	103	96	156	163	164	99
Cr	118	127	144	129	120	106	98	85	82	66	64	102	114	108	68
Co	19.9	13	12.5	14.8	14.6	23	12	17	28	16	19	13	16	9.8	16
Ni	63.9	45.3	56.5	61.3	57.8	44	49	49	46	36	36	53	53	48	39
Cu	6.89	17.5	16.1	12.1	13.8	16	6.7	29	50	10	29	0.3	0.5	0.8	5.7
Zn	86.3	33.6	32	55.4	52.8	18	52	90	88	83	79	39	80	50	46
Rb	215	255	283	174	179	132	158	107	230	124	121	97	105	76	128
Sr	42.2	32.9	34.8	47.5	50.2	44	45	49	64	822	260	59	81	60	143
Nb	18.6	16.8	19	17.1	17.7	12	14	16	14	11	9	11	14	12	9.7
Cs	12.7	12.5	14.4	8.62	8.46	4.9	7.7	8.9	16	5.2	6	8.7	6.8	4.1	4.9
Ba	708	598	1.19	567	568	556	411	339	1011	1928	404	407	322	453	418
Ta	1.13	1.01	1.2	1.06	1.11	1.8	2.4	2.6	2.6	1.2	0.9	1.9	2.2	1.7	1
Pb	16.9	7.13	5.61	3.51	4.33	4	4	6.8	17	60	13	3.9	5.2	4.8	5.8
Th	14.7	15.3	17.7	15.2	16.2	16	14	11	19	15	13	12	13	11	13
U	1.75	2.76	2.56	2.59	2.72	1.9	2	1.8	2.5	2.4	1.8	1.6	4	2.8	1.8
Zr	171	134	148	154	139	148	149	145	190	168	94	139	154	154	108
Hf	4.94	3.9	4.22	4.38	4.04	4.8	4.6	4	6.2	5.2	2.9	4.2	4.9	4.7	3.4
Y	27.9	22.9	28.1	26.5	25.2	24.27	18.24	25.13	25.38	21.58	13.98	19.24	19.82	15.39	11.17

Trace-Element Geochemistry.—Trace-element concentrations of Devonian siltstones and mudstones are reported in Table 4. In comparison with average upper continental crust, the concentrations of most trace elements are generally low. In siltstones the average relative concentration ratios of most elements lie between 0.1 and 1, except for Cr and Ni, which has consistently much higher average relative concentration values and low values of Rb, Zr, and Hf. Except for one mudstone sample, Rb and Zr are somewhat depleted as compared to the other elements, particularly Cr, Ba, Y, and Th (Fig. 7).

The high-field-strength elements such as Zr, Nb, Hf, Y, Th, and U are preferentially partitioned into melts during crystallization (Feng and Kerrich 1990), and as a result these elements are enriched in felsic rather than mafic rocks. Additionally, they are thought to reflect provenance compositions as a consequence of their generally immobile behavior (Taylor and McLennan 1985). The slightly higher contents of Nb, Y, U, and Th in the samples with higher ΣREE probably reflects a control by grain-size fractionation during transport, and may also suggest a contribution from a felsic source with a high concentration of these elements. The depletion of Zr and Hf in all analyzed samples could be related to the size variation and depletion of heavy-mineral fractions such as zircon in the Devonian sandstones.

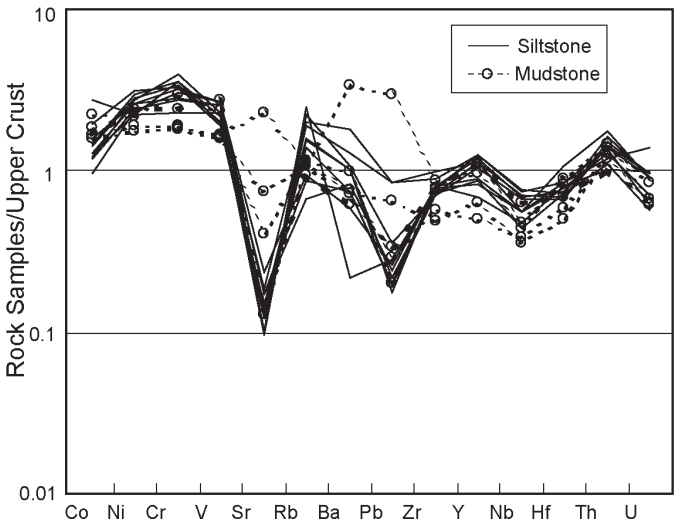

FIG. 7.—Multi-element normalized diagram for the Devonian siltstones and mudstones, normalized against average upper continental crust (Taylor and McLennan 1985).

Th, Sc, Zr, and REEs are particularly useful for provenance analysis, because their distribution is not significantly affected by diagenesis and metamorphism and is less affected by the heavy-mineral fraction than the case for elements such as Hf and Zr (Taylor and McLennan 1985; McLennan et al. 1990; Bhatia and Crook 1986). REEs and Th abundances are higher in felsic than in mafic igneous source rocks and in their weathered products, whereas Co, Sc, and Cr are more concentrated in mafic than felsic igneous rocks and their weathered products. Furthermore, ratios such as Eu/Eu*, La/Sc, Th/Sc, La/Co, Th/Co, and Cr/Th are significantly different in mafic and felsic source rocks and can therefore reflect provenance information of sedimentary rocks (Condie and Wronkiewicz 1990; Cullers and Podkovyrov 2000; Taylor and McLennan 1985). In our study, the Eu/Eu*, La/Sc, Th/Sc, La/Co, Th/Co, and Cr/Th values of the Devonian siltstones and mudstones are similar to the values for sediments derived from felsic source rocks compared with mafic source rocks (Table 5), suggesting that these Devonian sediments were probably derived from felsic sources.

Cr is a useful element in identifying accessory detrital components such as chromite, commonly derived from mafic to ultramafic sources including ophiolites, not readily recognized by petrography alone. The average Cr content of the upper continental crust is 83 ppm. (McLennan 2001). Cr values of the studied samples vary from 64 ppm to 144 ppm, and the average Cr/Th ratio (mean 7.1, N = 15) of the studied samples is lower than the average upper-continental crust value (7.8; McLennan 2001). The high Cr concentration in the studied samples probably results from chromite, indicating that mafic to ultramafic rocks probably provided some detritus for the Devonian deposits.

Discrimination of tectonic settings on the basis of La, Th, Zr, and Sc was proposed by Bhatia and Crook (1986); distinctive fields for four environments—island arc, continental arc, active continental margin, and passive margin—are recognized on ternary plots La-Th-Sc and Th-Sc-Zr/10. All of the Devonian samples fall in the continental-arc field of La-Th-Sc and Th-Sc-Zr/10 diagrams (Fig. 8), whereas most studied samples scatter over the active-continental-margin and continental-arc fields in the La-Th diagram.

TABLE 5.—*Range of elemental ratios of Devonian sandstones in this study compared to ratios in similar fractions derived from felsic rocks, mafic rocks, and upper continental crust.*

Element ratio	Range of analyzed samples[1]	Range of sediment from felsic source[2]	Range of sediment from mafic source[3]	Upper Continental crust[4]
Eu/Eu*	0.51–0.8	0.40–0.94	0.71–0.95	0.63
La/Sc	1.95–3.27	2.50–16.3	0.43–0.86	2.21
Th/Sc	0.68–1.07	0.84–20.5	0.05–0.22	0.79
La/Co	1.53–4.23	1.80–13.8	0.14–0.38	1.76
Th/Co	0.65–1.63	0.67–19.4	0.04–1.40	0.63
Cr/Th	4.32–9.82	4.00–15.0	25–500	7.76

[1] This study; [2] Cullers and Podkovyrov (2000); [3] Taylor and McLennan (1985).

Both these discrimination diagrams and trace-element ratios suggest that the provenance tectonic setting of the Devonian sediments, which were deposited in the Xicheng Basin, was a continental arc.

Rare-Earth Elements.—The REEs represent well-established provenance indicators (McLennan et al. 1990; McLennan et al. 1993; McLennan 2001). Table 6 shows the results of REE analyses; the chondrite-normalized patterns for the Shujiaba Group are in Figure 9A, and for the Dacaotan and Xihanshui groups in Figure 9B, compared with the REE patterns of sandstones derived from the Java, Peru–Chile, and Middle America continental arcs (McLennan et al. 1990). ΣREE concentrations vary widely in the Devonian rocks (ΣREE ~ 13–29), and they are less than the value of the average upper continental crust (~ 143; Taylor and McLennan 1985). All analyzed samples show slightly LREE-enriched and relatively flat HREE patterns with a negative Eu anomaly (Eu/Eu* = 0.5–0.8), except for two samples of the Xihanshui Group that have pronounced negative Tb and Tm anomalies (Fig. 9B). Devonian samples with REE patterns similar to those of modern deep-sea turbidites from continental arcs suggest that the Devonian rocks were derived from a continental arc and deposited in a forearc basin.

Paleocurrent Indicators

Paleocurrent indictors in sedimentary rocks provide key information on sediment deposited pathways. Abundant and diverse paleocurrent indicators in the Devonian deposits from the Xicheng Basin, such as cross lamination and ripple lamination, imbrication of gravels, flute casts, and various tool marks, yield consistent paleocurrent directions (Fig. 10).

In the northern basin, cross-bedding (Dacaotan area) and imbricated clasts (Gucheng area) of the Dacaotan Group indicate a uniform axial sedimentary transport from N and NE to S and SW. Ripple lamination and flute marks of the Shujiaba Group indicate sediment transport from north to south. Jin and Li (1997) studied flute casts of the Shujiaba Group near Yacheng and suggested that initially southward flow which diverged into branches flowing eastward and westward. Cross-lamination indictors also support these directions (Du 1997). These results imply that a southward-inclined slope developed during deposition of the Shujiaba Group.

In the northeast of the Mianxian area, ripple lamination points to southward transport. However, small-scale cross-lamination in the Xihanshui Group around Wujiashan shows two opposite directions: southward and northward (Fig. 10). Zuo (1984) studied the paleocurrent indictors in the Wujiashan area and also reported two different paleocurrent directions along the Xihe–Wujiashan trend (bottom left in Fig. 3). These results demonstrate that basement uplift controlled paleocurrent directions and supplied some clastic sediment to the basin. Around Wujiashan, clastic sandstone and conglomerate detritus, together with early Paleozoic metamorphic volcanic rocks (Zuo 1984; Feng et al. 2003), further demonstrate that basement provided some detritus to the Devonian basin.

Although Mesozoic–Cenozoic strike-slip motion occurred at different crustal levels, they were formed as result of the collision between the SCB and the NCB (Wang et al. 2003; Ratschbacher et al. 2003; Mattauer et al. 1985). Paleomagnetic data indicate that the movement of the SCB towards the NCB involved ~ 70° of clockwise rotation (Zhao and Coe 1987) and the Qinling ocean was not closed until the Late Jurassic (Enkin et al. 1992), with the result that the collision progressed from east to west. The Qinling orogen continued to be shortened in a north–south direction during Mesozoic collision. Although Mesozoic tectonism may have modified the Devonian paleocurrent indicators, nearly all of the data

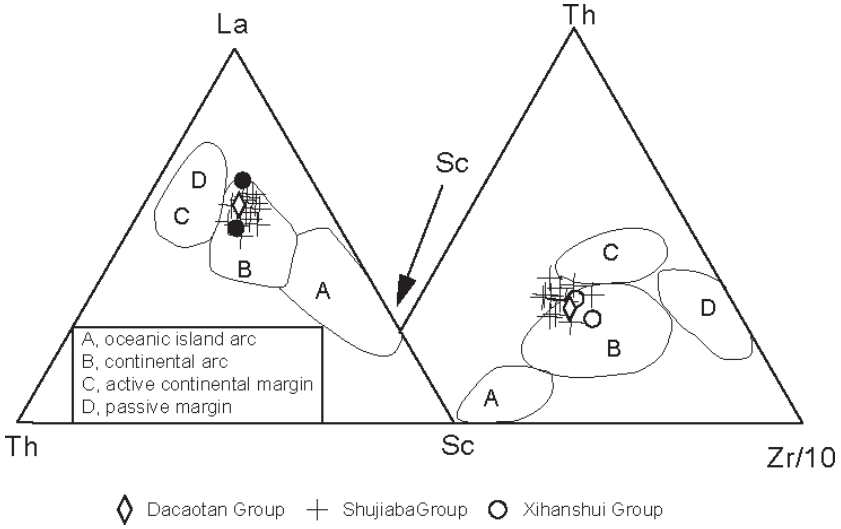

FIG. 8.—Tectonic discrimination diagrams for sandstones (after Bhatia and Crook 1986).

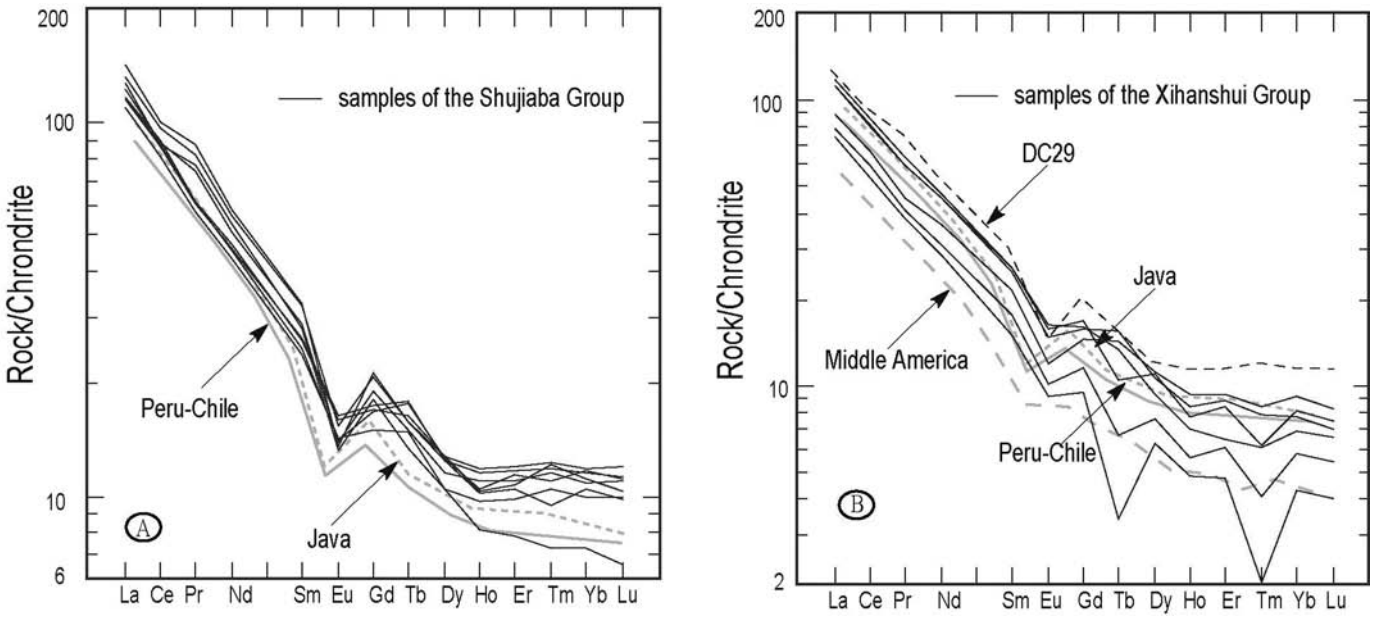

FIG. 9.—Chondrite-normalized rare-earth-element plots for the Devonian siltstones and mudstones. Chondrite normalization values are from Taylor and McLennan (1985). **A)** The Shujiaba Group; **B)** The Xihanhui and Dacaotan groups. Gray lines represent REE patterns of the turbidites from Mid-American, Peru–Chile, and Java continental arcs (McLennan et al. 1990).

point consistently to a northward provenance except for some around Wujiashan.

In summary, detrital data from the sandstones imply that a continental arc was the main provenance, but a suture belt and accretionary prism also provided some material. Major-element analysis suggests that the Devonian rocks were derived mainly from a continental arc, but an oceanic island arc cannot be excluded as a possible provenance. Trace-element geochemistry demonstrates that felsic rocks were the main source of the Devonian rocks. However, a high Cr concentration suggests that abundant chromite in the Devonian rocks was derived from mafic or ultramafic rocks. REE patterns further suggest that the Devonian rocks were derived from a continental arc and deposited in a forearc setting.

TABLE 6.—*Rare-earth-element concentrations in ppm for siltstones and mudstones of the Xicheng Basin.*

Sample	DC29	SH15	SH16	SH17	SH18	SH19	SH20	SH21	SH22	XH7	XH8	XH9	XH10	XH11	XH12
La	45.4	46.7	52.4	48.7	44.9	42.23	40.27	42.53	42.97	32.65	29.1	41.04	43.04	41.48	27.3
Ce	88.4	83.9	96.4	92.1	84.4	82.15	77.75	83.4	85.33	63.3	55.95	78.37	81.79	77.49	50.88
Pr	10.3	10.5	12	11.2	10.1	8.258	7.882	8.412	8.367	6.253	5.644	8.018	8.652	8.016	5.3
Nd	37.8	37.9	41.7	40.1	36.3	32.58	30.79	33.65	32.18	25.97	22.1	32.15	33.45	32.27	20.4
Sm	6.94	6.53	7.58	7.43	6.7	6.113	5.497	6.03	5.762	4.944	4.098	5.811	5.995	5.981	3.489
Eu	1.3	1.16	1.18	1.34	1.21	1.42	1.245	1.39	1.23	1.032	0.881	1.29	1.382	1.412	0.799
Gd	6.24	5.56	6.56	6.37	5.81	5.319	4.614	5.227	5.141	4.47	3.526	4.855	5.182	4.863	2.906
Tb	0.92	0.78	0.92	0.92	0.87	1.039	0.86	0.951	1.028	0.83	0.388	0.898	0.605	0.78	0.198
Dy	4.7	3.98	4.85	4.73	4.41	4.752	3.998	4.856	4.789	4.222	2.89	4.058	4.192	3.533	2.37
Ho	0.99	0.83	1.01	0.98	0.93	0.866	0.688	0.883	0.89	0.785	0.476	0.715	0.661	0.596	0.408
Er	2.91	2.44	2.98	2.91	2.72	2.61	1.945	2.67	2.827	2.307	1.511	2.188	2.097	1.601	1.179
Tm	0.43	0.37	0.44	0.42	0.41	0.335	0.26	0.431	0.392	0.301	0.145	0.28	0.218	0.214	0.073
Yb	2.85	2.46	2.93	2.88	2.7	2.6	1.793	2.753	2.894	2.272	1.421	1.939	2.018	1.705	1.067
Lu	0.44	0.38	0.46	0.43	0.42	0.375	0.251	0.394	0.425	0.318	0.204	0.266	0.285	0.25	0.153
(LREE/HREE)	9.69	11.04	10.43	10.16	9.98	9.57	11.26	9.58	9.50	8.59	11.07	10.88	11.33	12.20	12.85
ΣREE	27.72	24.49	28.91	28.41	26.18	25.429	21.151	25.585	25.378	21.481	15.54	22.3	22.635	20.935	12.642
Eu/Eu*	0.60	0.59	0.51	0.60	0.59	0.76	0.76	0.76	0.69	0.67	0.71	0.74	0.76	0.80	0.77
Cr/Th	8.03	8.30	8.14	8.49	7.41	6.63	7.00	7.73	4.32	4.40	4.92	8.50	8.77	9.82	5.23
Cr/Ni	1.85	2.80	2.55	2.10	2.08	2.41	2.00	1.73	1.78	1.83	1.78	1.92	2.15	2.25	1.74
Cr/V	1.03	0.96	1.02	1.09	0.97	0.74	0.63	0.51	0.59	0.64	0.67	0.65	0.70	0.66	0.69
Y/Ni	0.44	0.51	0.50	0.43	0.44	0.55	0.37	0.51	0.55	0.60	0.39	0.36	0.37	0.32	0.29
Th/Sc	0.84	0.78	0.83	0.84	0.84	1.07	0.82	0.85	1.00	1.07	1.00	0.71	0.68	0.69	0.93
Th/U	8.40	5.54	6.91	5.87	5.96	8.42	7.00	6.11	7.60	6.25	7.22	7.50	3.25	3.93	7.22
Th/Co	0.74	1.18	1.42	1.03	1.11	0.70	1.17	0.65	0.68	0.94	0.68	0.92	0.81	1.12	0.81
La/Y	1.63	2.04	1.86	1.84	1.78	1.74	2.21	1.69	1.69	1.51	2.08	2.13	2.17	2.70	2.44
La/Co	2.28	3.59	4.19	3.29	3.08	1.84	3.36	2.50	1.53	2.04	1.53	3.16	2.69	4.23	1.71
La/Sc	2.61	2.39	2.45	2.68	2.31	2.82	2.37	3.27	2.26	2.33	2.24	2.41	2.27	2.59	1.95

Eu* is equal to the square root of the sum of chondrite-normalized Sm and Gd. That is Eu* = (Sm normalized + Gd normalized) 1/2.

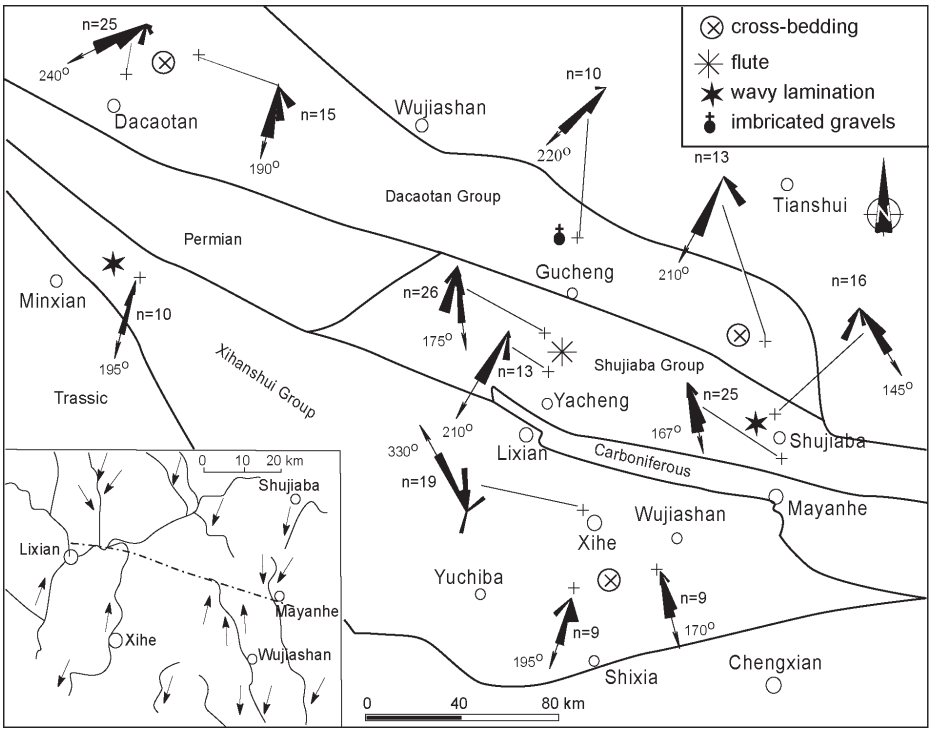

FIG. 10.—Paleocurrent indicators of the Devonian System in the Xicheng Basin. Inset in the left corner is after from Zuo (1984).

Paleocurrent indictors point to derivation from a continental arc to the north. All of this evidence demonstrates that the Qinling arc in the North Qinling was most probably the major source of the Devonian clastic material, but remains unclear whether the SCB also provided some detritus.

TECTONIC SETTING OF THE XICHENG BASIN

Collision of the NCB with the SCB in the Middle–Late Triassic is indicated by the following data in the Qinling orogen: paleomagnetic data (Zhao and Coe 1987; Enkin et al. 1992), ultra-high-pressure rocks (Ames et al. 1993; Okay and Sengör 1992; Ye et al. 2000; Hacker et al. 2004) and widespread collision-related granites (Shang and Yan 1988; Sun et al. 2002).

At ~ 490–470 Ma, an intraoceanic arc consisting of the Danfeng and Erlangping groups (Sun et al. 1996; Xue et al.1996a, 1996b; Reischmann et al. 1990; Kroner et al. 1993) was formed by northward subduction of the Qinling ocean and then accreted to the southern margin of the NCB (here termed the Qinling arc; Fig. 11). Geochemical and isotopic data demonstrate that metabasic volcanic rocks at Tianshui have island arc signatures and a zircon U–Pb age of 507 ± 3.0 Ma (Pei et al. 2005). Lu et al. (2003) obtained U–Pb zircon ages of 514 ± 1.3 Ma and 523 ± 26 Ma for arc-type volcanic rocks near the Fengxian and Shangnan areas, respectively (Fig. 1B). Eclogites and their granitic gneiss host rocks in the Shangnan area have a SHRIMP U–Pb zircon age of 507 ± 38 Ma (Yang et al. 2002). To the west, zircons from a magmatic arc and eclogites along the northern margin of Qaidam terrane have TIMS and SHRIMP U–Pb ages of 486 ± 13 Ma (Li et al. 1999), 496 ± 7.6 to 445 ± 15.3 Ma (Wu et al. 2001), and 495–440 Ma (Yang et al. 2002). Following emplacement of this intraoceanic arc belt, a continental arc was built along the southern margin of the NCB from ~ 438–395 Ma (Hacker et al. 2004), which provided some clastic detritus deposition (Gao et al. 1995). Therefore, Devonian forearc rocks contain abundant metamorphic detritus (Mattauer et al. 1985) from the Qinling unit and ~ 780 Ma and ~ 1.0 Ga detrital zircons, and deposition during the Silurian–Devonian before ~ 400 Ma, erosion and deposition of 350–440 Ma arc rocks followed by a low-temperature Triassic overprint (Ratschbacher et al. 2003). This suggests that a ~ 400 Ma Andean-type continental arc was built along the southern margin of the NCB (Ratschbacher et al. 2003; Xiao et al. 1999; Zhou et al. 1995; Zhai et al. 1998; Li and Sun 1995; Wang et al. 2002) and probably provided some detritus for the deposition. Significantly, the local absence of Upper Ordovician (~ 445 Ma) through Lower Carboniferous (~ 350 Ma) rocks from the NCB in the margin of the Qinling orogen probably reflects uplift related to the formation of this Andean-style active continental margin arc (Hacker et al. 2004).

Paleomagnetic data (Zhao and Coe 1987; Enkin et al. 1992) suggest that the NCB and SCB moved farther apart in the Middle Permian to Middle–Late Triassic, but then approached each other and underwent ~ 70° of relative rotation between Middle–Late Triassic and Early–Middle Jurassic times (Zhao and Coe 1987; Gilder et al. 1999), demonstrating that the convergence between the SCB and the NCB was not homogeneous along strike and that the exhumation in the eastern Qinling was considerable. Therefore, the arc in the western part of the Qinling orogen was not uplifted sufficiently to expose its batholithic core and provide deep-crustal granitoid fragments for the basin; abundant metamorphic and sedimentary detritus in the Xicheng Basin was probably derived from the cover of the continental arc. Sandstone samples plot within the overlap fields of an accretionary prism and a suture belt on the Lm-Ls-Lv diagram defined by Dickinson and Suczek (1979) (Fig. 5), suggesting that the Erlangping and Heihe arc–ophiolite assemblages provided detritus for the Devonian sediments. The higher Cr content of sandstones and mudstones also supports this idea. The sedimentary–volcanic cover of the Qinling orogen, as in Wujiashan, was eroded by uplift. The basement was exposed and eroded to provide some detritus for the basin.

CONCLUSIONS

Petrographic and geochemical data from the Devonian rocks of the Xicheng Basin suggest that they were derived mainly from a continental

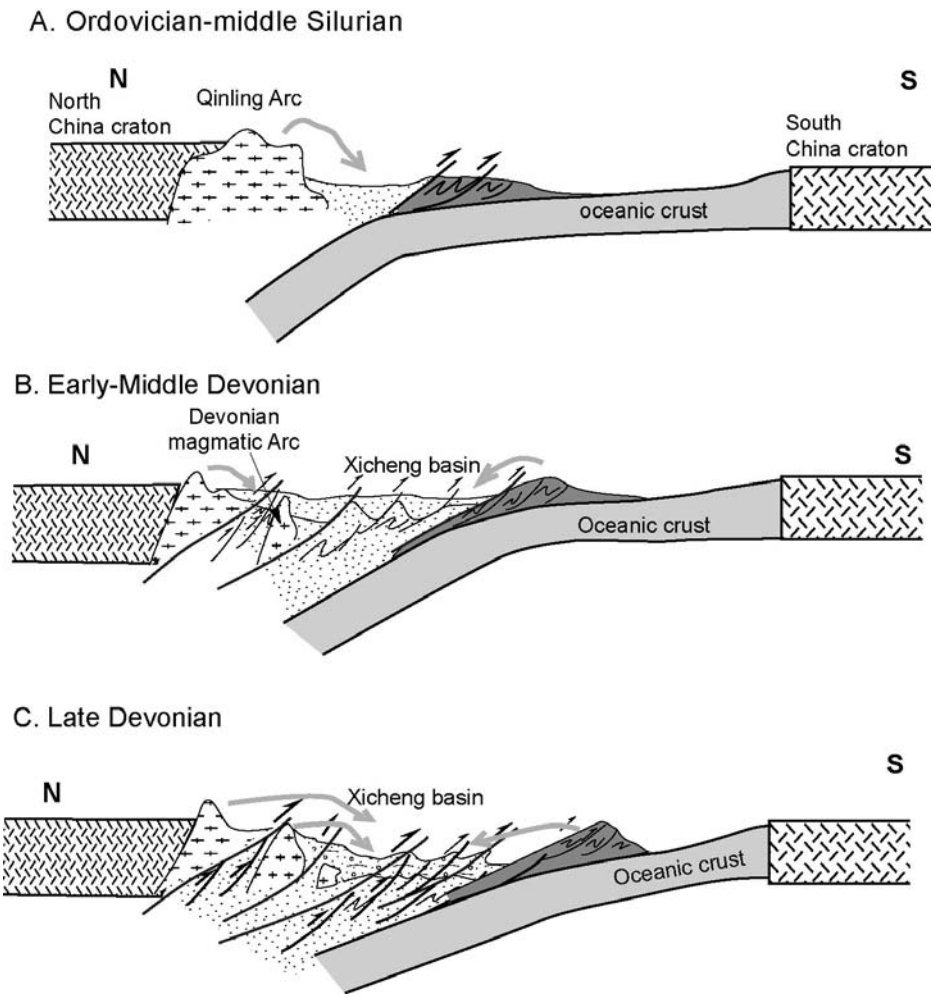

FIG. 11.—Sequential diagram showing the evolution of the late Paleozoic forearc basin in the Qinling orogen. **A)** Late Silurian to Early Devonian. **B)** Middle Devonian. **C)** Late Devonian.

arc. Paleocurrent indicators demonstrate that this arc was located on the northern margin of the basin. Except for some detritus originating from a local basement high, we do not know whether the SCB also provided some detritus for the Xihanshui Group.

The detrital composition of the sandstones demonstrates that the arc was not deeply exhumed, because it supplied abundant sedimentary and metamorphic lithic grains to the basin. Trace-element data suggest that felsic rocks provided the main source of the Devonian rocks. A high Cr concentration implies that mafic and ultramafic rocks were exposed in the source area and provided chromite for the basin. Rare-earth-element data of the Devonian fine-grained clastic rocks are similar to turbidites associated with modern continental arcs, which means that the Devonian deposits were deposited not in a foreland basin or passive margin, but rather in a forearc setting.

We interpret the available geological, geochemical, and geochronological data to indicate that there was an ~ 400 Ma regional magmatic event along the south margin of the NCB that was responsible for formation of an Andean-type continental margin which resulted in the regional metamorphism, sedimentation, and tectonism. This volcanic-magmatic arc and its associated accretionary wedge and forearc basin developed on a relatively long time period and record a complicated continuous orogenic process during oblique subduction of the Qinling ocean before the final collision of the SCB and NCB in the early Mesozoic. The presence of Devonian sandstones with few magmatic fragments suggests that this continental arc was not uplifted and exhumed strongly enough to expose its batholithic core.

ACKNOWLEDGMENTS

This paper represents part of a Ph.D. thesis by the first author, funded by the Geological Surveying Project of China DKD2001002 and NSFC 49972074, 40334044. Kathleen Marsaglia, Stephan Graham, and Bradley Ritts are thanked for providing constructive and helpful reviews. Kitty Milliken, Melissa Lester, and John B. Southard are also thanked for corrections and giving us self-confidence. Brian Windley kindly read the manuscript, and all the corrections are appreciated. We think C.-F. Jiang for discussion, and X.-X. Meng, J.-Q. Liu, and C.-Q. Su for field guidance in 2002.

REFERENCES

AMES, L.G., TILTON, G.R., AND ZHOU, G.Z., 1993, Timing of the Sino–Korea and Yangtze cratons: U–Pb zircon dating of coesite-bearing eclogites: Geology, v. 21, p. 339–342.

B.G.M. GANSU (THE 7TH GEOLOGICAL TEAM OF THE BUREAU OF GEOLOGY AND MINERAL RESOURCES OF GANSU PROVINCE), 1982, Geological and Mineral Mapping and Report of Tianshui Area, 1:200000 (in Chinese).

B.G.M. SHAANXI (GEOLOGICAL SURVEY TEAM OF THE BUREAU OF GEOLOGY AND MINERAL RESOURCES OF SHAANXI PROVINCE), 1999, Geological Map of the Liuba, (~ –48-E015020), 1:50000 (in Chinese).

B.G.M. Shaanxi (Geological Survey Team of the Bureau of Geology and Mineral Resources of Shaanxi Province), 1994, Geological Maps of the Yaoping (~ –48-92-D), Baishuijiang (~ –48-93-A), Shangliangheko (~ –48-93-B), Xujiaping (~ –48-93-C) and Lianghekou (~ –48-93-D), 1:50000 (in Chinese).

BHATIA, M.R., 1983, Plate tectonics and geochemical composition of sandstones: Journal of Geology, v. 91, p. 611–627.

BHATIA, M.R., AND CROOK, K.A.W., 1986, Trace element characteristics of greywackes and tectonic setting discrimination of sedimentary basins: Contributions to Mineralogy and Petrology, v. 92, p. 181–193.

Cao, X., Zhang, R., and Zhang, H., 1990, On stratigraphy and sedimentary environment of important ore-bearing horizon in Devonian Period, Qinling–Dabashan area, China: Chinese Academy of Geological Science, Xi'an Institute of Geological Mineralogy Research, Bulletin, v. 23, p. 1–124.

Collinson, J.D., 1986, Alluvial sediments, *in* Reading, H.G., ed., Sedimentary Environments and Facies: Oxford University, Blackwell Scientific, p. 20–62.

Condie, K., and Wronkiewicz, D.J., 1990, The Cr/Th ratio in Precambrian pelites from the Kaapvaal craton as an index of craton evolution: Earth and Planetary Science Letters, v. 97, p. 256–267.

Cullers, R.L., and Podkovyrov, V.N., 2000, Geochemistry of the Mesoproterozoic Lakhanda shale in southeastern Yakutia, Russia: Implications for mineralogical and provenance control, and recycling: Precambrian Research, v. 104, p. 77–93.

Dickinson, W.R., 1970, Interpreting detrital modes of graywacke and arkose: Journal of Sedimentary Petrology, v. 40, p. 695–707.

Dickinson, W.R., 1982, Compositions of sandstones in Circum-Pacific subduction complexes and forearc basins: American Association of Petroleum Geologists, Bulletin, v. 66, p. 121–137.

Dickinson, W.R., 1985, Interpreting provenance relations from detrital modes of sandstones, *in* Zuffa, G.G., ed., Provenance of Arenites: Dordrecht, D. Reidel, p. 333–361.

Dickinson, W.R., and Suczek, C.A., 1979, Plate tectonics and sandstone compositions: American Association of Petroleum Geologists, Bulletin, v. 63, p. 2164–2182.

Du, Y., 1997, Devonian sedimentary geology of Qinling orogenic belt, Wuhan: China University of Geosciences Press, 130 p (in Chinese with English abstract).

Enkin, R.J., Yang, Z., Chen, Y., and Courtillot, V., 1992, Paleomagnetic constraints on the geodynamic history of the major blocks of China from Permian to present: Journal of Geophysical Research, v. 97, p. 13953–13989.

Feng, R., and Kerrich, R., 1990, Geochemistry of fine-grained clastic sediments in the Archean Abitibi greenstone belt, Canada: Implications for provenance and tectonic setting: Geochimica et Cosmochimica Acta, v. 54, p. 1061–1081.

Feng, Y., Cao, X., and Zhang, E., 2003, Fragment, process and mechanism of the western Qinling orogenic belt: Xi'an Cartographic Press, 263 p (in Chinese).

Gao, S., Zhang, B.-R., Gu, X.-M., Xie, Q.-L., Gao, C.-L., and Guo, X.-M., 1995, Silurian–Devonian provenance changes of South Qinling basins: implications for accretion of the Yangtz (South China) to the North China cratons: Tectonophysics, v. 250, p. 183–197.

Gilder, S.A., Leloup, P.H., Courtillot, V., Chen, Y., Coe, R.S., Zhao, X., Xiao, W., Halim, N., Cogne, J.-P., and Zhu, R., 1999, Tectonic evolution of the Tancheng–Liujiang (Tan–Lu) fault via Middle Triassic to Early Cenozoic paleomagnetic data: Journal of Geophysical Research, v. 104, p. 15365–15390.

Graham, S.A., Ingersoll, R.V., and Dickinson, W.R., 1976, Common provenance for lithic grains in Carboniferous sandstones from Ouachita Mountains and Black Warrior basin: Journal of Sedimentary Petrology, v. 46, p. 620–632.

Hacker, B.R., Ratschbacher, L., Webb, L., Ireland, R., Walker, D., and Dong, S., 1998, U/Pb zircon ages constrain the architecture of the ultrahigh-pressure Qinling–Dabie Orogen, China: Earth and Planetary Science Letters, v. 161, p. 215–230.

Hacker, B.R., Ratschbacher, L., and Liou, J.G., 2004, Subduction, collision and exhumation in the ultrahigh-pressure Qinling–Dabie orogen, *in* Malpas, J., Fletcher, C.J.A., Ali, J.R., and Aitchison, J.C., eds., Aspects of the Tectonic Evolution of China: Geological Society of London, Special Publication 226, p. 157–175.

Hsü, K.J., Wang, Q., Li, J., Zhou, D., and Sun, S., 1987, Tectonic evolution of the Qinling Mountains, China: Eclogae Geologicae Helvetiae, v. 80, p. 735–752.

Huo, F., and Li, Y., 1995, Evolution of the Western Qinling orogenic belt: Acta Geologica of Gansu, v. 5, n. 1, p. 1–15 (in Chinese with English abstract).

Ingersoll, R.V., and Suczek, C.A., 1979, Petrology and provenance of Neogene sand from Nicobar and Bengal Fans, DSDP Sites 211 and 218: Journal of Sedimentary Petrology, v. 49, p. 1217–1228.

Jin, H., and Li, Y., 1997, Distribution characteristics of trace fossil group in turbidite measure (Devonian) in the northern belt of West Qinling Mountains: Acta Sedimentologica Sinica, v. 15, n. 1, p. 13–19.

Kroner, A., Zhang, G.W., and Sun, Y., 1993, Granulites in the Tongbai area, Qinling belt, China: geochemistry, petrology, single zircon geochronology, and implications for the tectonic evolution of eastern Asia: Tectonics, v. 12, p. 245–255.

Lerch, M.F., Xue, F., Kroner, A., Zhang, G.W., and Todt, W., 1995, A Middle Silurian–Early Devonian magmatic arc in the Qinling Mountains of central China: Journal of Geology, v. 103, p. 437–449.

Li, C., Liu, Y., Zhu, B., Feng, Y., and Wu, H., 1978, Tectonic history of the Qinling and Qilian mountains, *in* Papers on Geology for International Exchange, Volume 1, Regional Geology and Geological Mechanics: Beijing, Geological Publishing House, p. 174–187 (in Chinese).

Li, J., Cao, X., and Yang, J., 1994, Sedimentation and evolution of Phanerozoic oceanic basin in the Qinling orogenic belt: Beijing, Geological Publishing House, 206 p (in Chinese).

Li, S., and Sun, W., 1995, A middle Silurian–Early Devonian magmatic arc in the Qinling Mountains of central China: a discussion: Journal of Geology, v. 104, p. 501–503.

Li, Y., 1989, The new advance on Xihanshui Group: Northwest Geology, v. 3, p. 59–63 (in Chinese with English abstract).

Liang, Z., 1994, The feature of geology and geochemistry and tectonic setting of the Danfeng Group metavolcanite in Tianshui region, Gansu province: Acta Geologica of Gansu, v. 3, n. 1, p. 72–78.

Liu, B., Xiao, J., and Zhou, Z., 1992, Geological Papers of Paleo-continental margin: Wuhan, China University of Geosciences Press, 142 p (in Chinese with English Abstract).

Lu, S., Li, H., and Chen, Z., 2003, Characteristics, sequence and ages of Neoproterozoic thermo-tectonic events between Tarim and Yangtze blocks: Earth Science Frontiers, v. 10, p. 321–326.

Marsaglia, K.M., 1991, Provenance of sands and sandstones from the Gulf of California, a rifted continental arc, *in* Fisher, R.V., and Smith, G.A., eds., Sedimentation in Volcanic Settings: SEMP, Special Publication 45, p. 237–248.

Marsaglia, K.M., 1992, Provenance and petrology of volcaniclastic sands recovered on ODP Leg 126, the Izu–Bonin arc: Proceedings of the Ocean Drilling Program, Scientific Results, v. 126, p. 139–154.

Marsaglia, K.M., and Ingersoll, R.V., 1992, Compositional trends in arc-related, deep-marine sand and sandstone: A reassessment of magmatic-arc provenance: Geological Society of America, Bulletin, v. 104, p. 1637–1649.

Mattauer, M., Matte, P., Malavieille, J., Tapponnier, P., Maluski, H., Xu, Z., Lu, Y., and Tang, Y., 1985, Tectonics of the Qinling belt: Build-up and evolution of eastern Asia: Nature, v. 317, p. 496–500.

Matte, P., Tapponnier, P., Arnaud, N., Bourjot, L., Avouac, J.P., Vidal, P., Liu, Q., Pan, Y.S., and Wang, Y., 1996, Tectonics of Western Tibet, between the Tarim and the Indus: Earth and Planetary Science Letters, v. 142, p. 311–330.

McLennan, S.M., 1989, Rare earth elements in sedimentary rocks: Influence of provenance and sedimentary process: Mineralogical Society of America, Reviews in Mineralogy, v. 21, p. 169–200.

McLennan, S.M., 2001, Relationships between the trace element composition of sedimentary rocks and upper continental crust: Geochemistry, Geophysics, Geosystems, v. 2, 2000GC000109.

McLennan, S.M., Taylor, S.R., McCulloch, M.T., and Maynard, J.B., 1990, Geochemical and Nd–Sr isotopic composition of deep-sea turbidites: Crustal evolution and plate tectonic associations: Geochimica et Cosmochimica Acta, v. 54, p. 2015–2050.

McLennan, S.M., Hemming, S., McDaniel, D.K., and Hanson, G.N., 1993, Geochemical approaches to sedimentation, provenance and tectonics, *in* Johansson, M.J., and Basu, A., eds., Processes Controlling the Composition of Clastic Sediments: Geological Society America, Special Paper 284, p. 21–40.

Meng, Q., and Zhang, G., 1999, Timing of collision of the North and South China blocks: controversy and reconciliation: Geology, v. 27, p. 123–126.

Meng, Q.-R., and Zhang, G.-W., 2000, Geologic framework and tectonic evolution of Qinling orogen, Central China: Tectonophysics, v. 323, p. 183–196.

Meng, Q., Yu, Z., and Mei, Z., 1997, Sedimentation and Development of the forearc basin at southern margin of North Qinling: Scientia Geologica Sinica, v. 32, p. 136–145.

Miall, A.D., 1992, Alluvial deposits, *in* Walker, R.G., and James, N.P., eds., Facies Models: Geological Association of Canada, p. 119–142.

Okay, A.I., and Şengör, A.M.C., 1992, Evidence for intracontinental thrust-related exhumation of the ultra-high-pressure rocks in China: Geology, v. 240, p. 411–414.

Pei, X.-Z., Li, Y., Lu, S.-N., Chen, Z.-H., Ding, S.-P., Hu, B., Li, Z.-C., and Liu, H.-B., 2005, Zircons U–Pb ages of the Guanzizhen intermediate-basic igneous complex in Tianshui area, West Qinling and their geological significance: Geological Bulletin of China, v. 24, p. 23–29 (in Chinese with English abstract).

Ratschbacher, L., Hacker, B.R., Calvert, A., Webb, L.E., Grimmer, J.C., McWilliams, M.O., Ireland, T., Dong, S., and Hu, J., 2003, Tectonics of the Qinling (Central China): tectonostratigraphy, geochronology, and deformation history: Tectonophysics, v. 366, p. 1–53.

Regional Surveying Team of Shaanxi Province, 1971, Stratigraphic Sequence of the Western Qinling Mountains, 57 p (in Chinese).

Reischmann, T., Kröner, A., Sun, Y., Yu, Z., and Zhang, G., 1990, Opening and closure of an early Paleozoic ocean in the Qinling orogenic belt, China: Terra Abstracts, v. 2, p. 55–56.

Ren, J.-S., Zhang, Z.-K., Niu, B.-G., and Liu, Z.-G., 1991, On the Qinling orogenic belt- integration of the Sino–Korean and Yangtze blocks, *in* Ye, L.-J., Qian, X.-L., and Zhang, G.-W., eds., A Selection of Papers Presented at the Conference on the Qinling Orogenic Belt: Northwest University Press, Xi'an, p. 99–110 (in Chinese with English abstract).

Roger, F., Arnaud, N., Gilder, S., Tapponnier, P., Jolivet, M., Brunel, M., Malavieille, J., Xu, Z., and Yang, J., 2003, Geochronological and geological constraints on Mesozoic suturing in east central Tibet: Tectonics, v. 22, n. 4, 1037, DOI: 10.1029/2002TC001466.

Schwab, M., Ratschbacher, L., Siebel, W., McWilliams, M., Minaev, V., Lutkov, V., Chen, F., Stanek, K., Nelson, B., Frisch, W., and Wooden, J.L., 2004, Assembly of the Pamirs: Age and origin of magmatic belts from the southern Tian Shan to the southern Pamirs and their relation to Tibet: Tectonics, v. 23, TC4002, DOI: 10.1029/2003TC001583.

Shang, R.J., and Yan, Z., 1988. Granites in Qinling and Bashan Mountains: Xi'an Jiaotong University Press, p. 1–85 (in Chinese with English abstract).

Su, J., and Huang, W., 2000, The features and time—discussion of the spore assemblages from Shujiaba Formation in West Qinling area: Acta Geologica of Gansu, v. 9, n. 1, p. 16–22 (in Chinese with English abstract).

Sun, W., Li, S., Sun, Y., Zhang, G., and Zhang, Z., 1996, Chronology and geochemistry of a lava pillow in the Erlangping Group at Xixia in the northern Qinling Mountains: Geology Reviews, v. 42, p. 144–153.

Sun, W., Li, S., Chen, Y., and Li, Y., 2002, Timing of synorogenic granitoids in the South Qinling, Central China: constraints on the evolution of the Qinling–Dabie orogenic belt: Journal of Geology, v. 110, p. 457–468.

Taylor, S.R., and McLennan, S.M., 1985. The Continental Crust; Its Composition and Evolution: Oxford University: Blackwell, p. 1–312.

Wang, E., Meng, Q., Burchfiel, B.C., and Zhang, G., 2003, Mesozoic large-scale lateral extrusion, rotation, and uplift of the Tongbai–Dabie Shan belt in east China: Geology, v. 31, p. 307–310.

Wang, T., 2003, Characters of the accretionary mélange belt in the south margin of the West Qinling, central China (Unpublished MSc thesis, in Chinese with English abstract). 54 p.

Wang, Z., Du, Y., and Cheng, S., 1995, Slope deposits and their tectonic significance of Permian rift-and-sag belt in Minxian area, west Qinling: Geoscience, v. 9, p. 300–310.

Wang, Z., Chen, H., and Hao, J., 1999, Preliminary determination of a late Paleozoic and Triassic fore-arc accretionary wedge in the South Qinling, *in* Chen, H., Hou, Q., and Xiao, W., eds., Collision Orogenic Belt: Beijing, Marine Press, p. 100–113 (in Chinese with English Abstract).

Wang, Z., Wang, T., Yan, Z., and Yan, Q., 2002, Late Paleozoic fore-arc accretionary piggyback type basin system in the south Qinling, Central China: Geological Bulletin of China, v. 21, p. 456–464 (in Chinese with English abstract).

Wu, C., Yang, J., Ireland, T., Wooden, J., Li, H., Wan, Y., and Shi, R., 2001, Zircon SHRIMP ages of Aolaoshan granite from the south margin of Qilianshan and its geological significance: Acta Petrologica Sinica, v. 17, n. 2, p. 215–221.

Xiao, P., Zhang, J., and Wang, H., 1999, The corrrelational study of various periods of volcanic rocks in Tangzang–Huangbeiyuan tectonic belt in Fengtai area, Shaanxi province: Geology of Shaanxi, v. 17, n. 2, p. 33–41 (in Chinese with English abstract).

Xiao, W.J., Windley, B.F., Chen, H., Zhang, G.C., and Li, J.L., 2002a, Carboniferous–Triassic subduction and accretion in the western Kunlun, China: implications for the collisional and accretionary tectonics of the northern Tibetan plateau: Geology, v. 30, p. 295–298.

Xiao, W.J., Windley, B.F., Hao, J., and Li, J.L., 2002b, Arc-ophiolite obduction in the Western Kunlun Range (China): implications for the Palaeozoic evolution of central Asia: Geological Society of London, Journal, v. 159, p. 517–528.

Xiao, W.J., Han, F.L., Windley, B.F., Yuan, C., Zhou, H., and Li, J.L., 2003, Multiple accretionary orogenesis and episodic growth of continents: Insights from the Western Kunlun Range, Central Asia: International Geology Review, v. 45, p. 303–328.

Xue, F., Kroner, A., Reischmann, T., and Lerch, F., 1996a, Paleozoic pre- and post-collision calc-alkaline magmatism in the Qinling orogenic belt, central China, as documented by zircon ages on granitoid rocks: Geological Society of London, Journal, v. 153, p. 409–417.

Xue, F., Lerch, M.F., Kroner, A., and Reischmann, T., 1996b, Tectonic evolution of the east Qinling Mountains, China, in the Paleozoic: a review and new tectonic model: Tectonophysics, v. 253, p. 271–284.

Yan, Z., 1985, Granitic rocks in Shaanxi Province, China: Xi'an Communications Institute Press, Xi'an (in Chinese), p. 1–321.

Yan, Z., 2002. Sedimentation and metallization of the late Paleozoic forearc basin in the West Qinling orogenic belt [PhD. Thesis]: Beijing, Chinese Academy of Science, 116 p (in Chinese with English Abstract).

Yan, Z., Wang, Z., Wang, T., and Yan, Q., 2002, Sedimentary environment and tectonic significance of the Dacaotan Group of the western Qinling Mountains: Geological Bulletin of China, v. 21, p. 505–515 (in Chinese with English abstract).

Yang, J., Xu, Z., Pei, X., Shi, R., Wu, C., Zhang, J., Li, H., Meng, F., and Rong, H., 2002, Discovery of diamond in North Qinling: evidence for a giant UHPM belt across central China and recognition of Paleozoic and Mesozoic dual deep subduction between North China and Yangtze plates: Acta Geologica Sinica, v. 75, p. 484–495.

Yang, Z., 1999, The accretional forearc structural zone and its evolutionary analysis in late Paleozoic in the middle part of Qinling area: Shannxi Geology, v. 17, n. 2, p. 1–6 (in Chinese with English Abstract).

Ye, K., Cong, B.L., and Ye, D.N., 2000, The possible subduction of continental material to depths greater than 200 km: Nature, v. 407, p. 734–736.

Ye, L., and Guan, S., 1944, Bulletin of geology, central south part of Gansu Province: Special Paper of the Geology, n. 19, 72 p (in Chinese).

Ye, X., 1986, On the occurrence of spore assemblages from the Shujiaba region of Tianshui County, Gansu and their stratigraphic significance: Chinese Academy of Geological Science, Xi'an Institute of Geological Mineralogy Resource, Bulletin, v. 13, p. 89–98 (in Chinese with English abstract).

Yin, A., and Nie, S., 1993, An indentation model for the north and south China collision and the development of the Tanlu and Honam Fault systems, eastern Asia: Tectonics, v. 12, p. 801–813.

Yu, Z., and Meng, Q., 1995, Late Paleozoic sedimentary and tectonic evolution of the Shangdan suture zone, Eastern Qinling, China: Journal of Southeast Asian Earth Science, v. 11, p. 237–242.

Zhai, X., Day, H.W., Hacker, B.R., and You, Z., 1998, Paleozoic metamorphism in the Qinling orogen, Tongbai Mountains, central China: Geology, v. 26, p. 371–374.

Zhang, C., Meng, Q., Yu, Z., and Zhang, G., 1997, Geochemical characteristics and tectonic implication of gravels in the Hubaohe conglomerates in the East Qinling: Acta Sedimentologica Sinica, v. 15, p. 115–119 (in Chinese with English abstract).

Zhang, C., Yang, R., Zhu, L., Jin, Z., and Yang, Z., 1999, The discovery of the Proterozoic Erathem in western Qinling and its significance: Journal of Stratigraphy, v. 22, p. 211–216 (in Chinese with English abstract).

Zhang, E., Niu, D., Huo, Y., Zhang, L., and Li, Y., 1993, Geologic–tectonic features of Qinling–Dabashan mountains and adjacent regions: Beijing, Geological Publishing House, 291 p (in Chinese with English abstract).

Zhang, G., Su, Y., Yu, Z., and Xue, F., 1988, The ancient active continental margin of the northern Qinling orogenic belt, *in* Zhang, G., ed., Formation and Evolution of the Qinling Orogen: Xi'an, Northwest University Press, p. 48–64 (in Chinese with English Abstract).

Zhang, G., Yu, Z., Sun, Y., Cheng, S., Li, T., Xue, F., and Zhang, C., 1989, The major suture zone of the Qinling orogenic belt: Journal of Southeast Asia Earth Science, v. 3, p. 63–76.

Zhang, H.-F., Gao, S., Zhang, B.-R., Luo, T.-C., and Lin, W.-L., 1995, Pb isotopes of granitoids suggest Devonian accretion of Yangtze (South China) craton of North China craton: Geology, v. 25, p. 1015–1018.

Zhang, W., Meng, X., and Hu, J., 1994, Tectonic characteristics and orogenic process in the joint of Qilian–North Qinling orogenic belts: Northeast University Press: Xi'an, 283 p (in Chinese with English Abstract).

Zhao, Z., and Coe, R.S., 1987, Paleomagnetic constraints on the collision and rotation of North and South China: Nature, v. 327, p. 141–144.

Zhou, D., Zhang, C., Han, S., Zhang, Z., and Dong, Y., 1995, Tectonic setting on the two different tectonics–magma complex of the East Qinling in early Paleozoic: Acta Petrologica Sinica, v. 11, n. 2, p. 115–126 (in Chinese with English abstract).

Zuo, G., 1984, Devonian tectonics—formational belts and crustal evolution in the western Qinling: Gansu Geology, v. 2, p. 99–109 (in Chinese with English abstract).

Received 1 July 2004; accepted 25 August 2005.

APPENDIX 1.—*Raw point-count data of Devonian sandstone samples from the Xicheng Basin.*

Sample	Qm	Qp	P	K	Lvv	Lvf	Lvmi	Lvl	Lvp	Lmv	Lmm	Lmt	Lma	Lmp	Lsa	Lsc	Lsch	Lsi	M	D	Carb	Misc
DC1	97	30	67	34	0	5	50	11	0	32	14	42	0	58	0	0	51	2	2	1	2	2
DC2	116	35	72	31	0	2	45	10	0	12	9	41	0	51	8	0	56	4	5	0	4	0
DC3	100	44	100	53	0	2	23	5	0	7	5	64	0	37	2	0	48	10	0	0	0	0
DC4	123	49	54	23	0	1	44	15	0	13	21	55	0	41	8	2	47	4	0	0	0	0
DC5	117	45	58	25	0	5	33	8	5	21	13	53	3	39	20	0	43	10	0	0	0	2
DC6	127	47	48	38	0	8	41	7	0	16	11	65	2	30	16	0	31	8	3	2	0	0
DC7	109	23	92	32	0	7	40	10	1	11	7	67	2	37	3	0	42	9	5	1	0	2
DC8	90	24	126	58	0	7	19	13	4	6	0	50	7	50	3	1	20	12	5	2	3	0
DC9	129	31	45	36	0	10	66	9	3	23	0	46	12	25	4	0	29	17	5	0	6	4
DC10	95	24	76	26	0	10	40	15	6	20	6	53	7	42	7	0	52	18	1	0	0	2
DC11	133	67	39	16	0	8	42	25	0	27	9	43	3	29	8	0	37	9	3	1	0	1
DC12	98	24	63	30	0	9	56	28	4	22	4	57	3	33	6	0	39	10	8	3	1	2
DC13	137	73	81	28	6	5	25	2	0	8	0	44	1	42	1	0	29	8	10	0	0	0
DC14	93	53	32	21	0	6	71	10	2	24	3	63	4	39	3	0	64	4	5	1	0	2
DC15	125	48	65	33	0	7	44	2	0	9	0	57	3	35	1	0	53	7	9	0	2	0
DC16	138	59	64	34	0	3	65	2	1	10	1	49	8	37	1	0	8	8	6	1	0	5
DC17	115	42	87	60	0	2	52	9	3	3	1	35	0	28	2	0	48	8	3	2	0	0
DC18	72	36	46	41	0	14	68	19	7	24	4	55	4	46	12	0	38	10	2	1	0	1
DC19	112	58	38	25	1	10	64	5	11	16	2	52	7	35	2	0	47	8	4	0	1	2
DC20	94	39	69	43	0	14	64	10	0	29	0	49	9	26	5	10	29	9	1	0	0	0
DC21	123	47	63	37	0	3	43	11	1	9	8	44	5	54	3	0	35	7	6	1	0	0
DC22	120	49	58	40	4	11	50	3	2	28	0	52	3	14	14	0	43	6	0	1	2	0
DC23	108	39	71	39	0	3	47	6	0	45	0	48	2	39	4	0	45	4	0	0	0	0
DC24	142	54	56	38	0	2	49	11	0	36	6	46	0	21	0	0	32	0	4	0	3	0
DC25	150	48	66	39	0	0	38	12	0	38	3	56	0	10	0	0	39	0	0	1	0	0
DC26	137	39	59	32	0	6	48	10	0	47	5	46	3	18	1	0	45	3	1	0	0	0
DC27	127	36	67	36	0	0	36	7	0	34	0	49	0	43	6	0	53	6	0	0	0	0
DC28	134	37	59	31	0	4	47	15	2	23	5	51	2	49	2	0	27	7	2	0	3	0
SH1	120	27	108	30	0	8	48	25	0	7	6	59	0	42	3	0	10	1	5	0	1	0
SH2	109	37	85	37	0	4	29	10	0	0	0	71	2	43	0	4	49	6	6	5	3	0
SH3	112	59	78	64	2	0	21	2	0	0	0	82	9	14	0	0	52	2	0	0	0	3
SH4	119	69	63	29	0	4	11	19	0	0	1	67	24	31	0	0	49	8	6	0	0	0
SH5	102	56	66	35	0	2	9	8	0	25	5	84	17	49	7	0	23	9	1	0	2	0
SH6	130	39	58	11	0	2	19	3	0	31	2	69	14	52	1	0	37	23	6	0	0	3
SH7	120	29	90	39	0	3	13	4	0	29	13	58	7	53	1	0	29	4	8	0	0	0
SH8	140	36	63	34	0	2	23	18	0	19	9	65	6	37	3	0	27	9	0	0	9	0
SH9	132	29	59	52	0	3	12	9	0	32	6	59	12	49	5	0	32	3	6	0	0	0
SH10	122	21	136	51	0	2	19	8	0	29	0	57	8	26	0	0	17	0	2	0	0	2
SH11	119	39	62	55	0	0	10	12	0	23	3	67	7	38	0	0	43	15	0	0	7	0
SH12	132	57	48	32	0	1	13	9	0	27	1	70	7	42	7	0	50	3	1	0	0	0
SH13	124	16	54	49	0	0	37	16	0	34	1	61	8	47	9	0	39	3	2	0	0	0
SH14	133	46	61	56	0	5	29	10	0	37	5	42	9	29	3	0	30	2	3	0	0	0
XH1	119	47	49	27	0	4	68	15	0	38	2	53	8	48	1	0	12	5	0	0	4	0
XH2	103	41	39	27	3	5	40	5	0	39	5	47	6	52	3	6	53	11	4	0	7	4
XH3	117	49	34	24	0	7	49	3	0	29	0	50	9	55	3	5	50	11	5	0	0	0
XH4	127	45	64	35	6	16	31	4	0	22	1	41	8	35	1	10	32	16	3	2	1	0
XH5	108	39	58	32	14	20	30	13	3	35	6	52	16	16	4	0	26	10	7	3	5	3
XH6	99	48	70	40	5	7	41	13	7	38	14	22	17	34	0	9	34	0	0	2	0	0